1
Electrochromic Metal Oxides: An Introduction to Materials and Devices

Claes-Göran Granqvist

1.1
Introduction

Electrochromic materials are able to change their properties under the action of an electrical voltage or current. They can be integrated in devices that modulate their transmittance, reflectance, absorptance or emittance. Electrochromism is known to exist in many types of materials. This chapter considers electrochromic metal oxides and devices based on these.

Figure 1.1 shows a generic electrochromic device comprising five superimposed layers on a single transparent substrate or positioned between two transparent substrates [1]. Its variable optical transmittance ensues from the electrochromic films, which change their optical absorption when ions are inserted or extracted via a centrally positioned electrolyte. The ion transport is easiest for small ions, and protons (H^+) or lithium ions (Li^+) are used in most electrochromic devices. Transparent liquid electrolytes as well as ion-containing thin oxide films were employed in early studies on electrochromics [2], but polymer electrolytes became of interest subsequently [3, 4] and paralleled the developments in electrical battery technology.

The ions are moved in the electrochromic device when an electrical field is applied between two transparent electrical conductors, as illustrated in Figure 1.1. The required voltage is only of the order of 1 V DC, so powering is, in general, easy and can be achieved by photovoltaics [5]. In small devices, the voltage can be applied directly to the transparent conductors but large devices – such as 'smart' windows for buildings – require 'bus bars', that is, a metallic frame partly or fully around the circumference of the transparent conducting thin film in order to achieve a uniform current distribution and thereby sufficiently fast and uniform colouring and bleaching. The transparent substrates are often of flat glass, but polymers such as polyethylene terephthalate (PET) or polycarbonate can also be used. The permeation of gas and humidity through foils may or may not be an issue for devices; barrier layers can be applied if needed [6].

An electrochromic device contains three principally different kinds of layered materials: The electrolyte is a pure *ion conductor* and separates the two

Electrochromic Materials and Devices, First Edition.
Edited by Roger J. Mortimer, David R. Rosseinsky and Paul M. S. Monk.

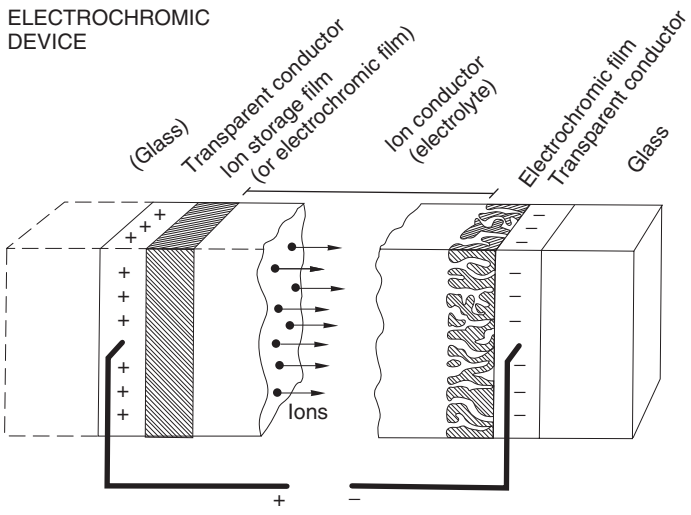

Figure 1.1 Generic five-layer electrochromic device design. Arrows indicate movement of ions in an applied electric field. From Ref. [1].

electrochromic films (or separates one electrochromic film from an optically passive ion storage film). The electrochromic films conduct both ions and electrons and hence belong to the class of *mixed conductors.* The transparent conductors, finally, are pure *electron conductors.* Optical absorption occurs when electrons move into the electrochromic film(s) from the transparent conductors along with charge-balancing ions entering from the electrolyte. This very simplified explanation of the operating principles for an electrochromic device emphasises that it can be described as an 'electrical thin-film battery' with a charging state that translates to a degree of optical absorption. This analogy has been pointed out a number of times but has only rarely been taken full advantage of for electrochromics.

Electrochromic devices have a number of characteristic properties that are of much interest for applications. Thus, they exhibit *open circuit memory*, just as electrical batteries do, and can maintain their optical properties and electrical charge for extended periods of time without drawing energy (depending on the quality of electrical insulation of the electrolyte). The *optical absorption can be tuned* and set at any level between states with minimum and maximum absorption. The *optical changes are slow* and have typical time constants from seconds to tens of minutes, depending on physical dimensions, which means that the optical changes can occur on a timescale comparable with the eyes' ability to light-adapt. Furthermore, the optical properties are based on processes on an atomic scale, so electrochromic windows can be *without visible haze*; this latter property has been documented in detailed spectrally resolved measurements of scattered light [7]. By combining two different electrochromic films in one device, one can adjust the optical transmittance and reach better *colour neutrality* than with a single

electrochromic film. Finally, the *electrolyte can be functionalised,* provided it is a solid and adhesive bulk-like polymer, so that the smart window combines its optical performance with spall shielding, burglar protection, acoustic damping, near-infrared damping and perhaps even more features.

This chapter is organised as follows: Section 1.2 serves as a background and gives some notes on early work on electrochromic materials and devices. Section 1.3 provides an in-depth discussion of EC materials and covers optical and electronic effects and, specifically, charge transfer in tungsten oxide. It also treats ionic effects with foci on the inherent nanoporosity in electrochromic oxides and on possibilities to augment the porosity by choosing appropriate thin-film deposition parameters. A number of concrete examples on the importance of the deposition conditions are reported, and Section 1.3 ends with a discussion of the electrochromic properties of tungsten–nickel oxide films across the full compositional range. Section 1.4 surveys properties of transparent conducting electrode materials as well as transparent electrolytes. Section 1.5 gives a background to electrochromic devices, specifically delineating a number of hurdles for practical device manufacturing as well as principles for some large-area devices. Conclusions are given in Section 1.6.

1.2
Some Notes on History and Early Applications

Electrochromism in thin films of metal oxides seems to have been discovered several times through independent work. A vivid description of electrically induced colour changes in thin films of tungsten oxide immersed in sulfuric acid was given in an internal document at the Balzers AG in Liechtenstein in 1953 (cited in a book on inorganic electrochromic materials [1]). Later work on W oxide films by Deb at the American Cyanamid Corporation during the 1960s yielded analogous results, which were reported in two seminal papers in 1969 and 1973 [8, 9]; these publications are widely seen as the starting point for research and development of electrochromic devices. Deb's early work was discussed in some detail much later [2, 10]. Another very important electrochromic oxide is Ni oxide, whose usefulness became clear in the mid-1980s [11, 12]. Parallel developments took place in the Soviet Union, and a paper from 1974 [13] quotes 'USSR Author's Certificates' and patents by Malyuk *et al.* dating back to 1963; this work dealt with Nb oxide films.

Early research on electrochromic materials and devices in the United States, Soviet Union, Japan and Europe was motivated by potential applications in *information displays*, and there were strong research efforts during the first half of the 1970s at several large companies. Generally speaking, these efforts became of less relevance towards the end of the 1970s, and liquid-crystal-based constructions then started to dominate the market for small displays. Electrochromic-based variable-transmission glass was of interest in the context of cathode ray tubes for some time [14]. At present, there is a strong resurgence in the interest

in electrochromic-based display-oriented devices (such as 'electronic paper'), and much research and development is devoted to organics-based full-colour electrochromic displays with excellent viewing properties, cheap printable electrochromic 'labels' and, very recently, to 'active' authentication devices [15].

Electrochromic-based *rear-view mirrors* for cars and trucks provide another applications area, and it appears that research and development goes back to the late 1970s [16]. However, the market for 'active' rear-view mirrors was largely taken by a device design that is not identical to the one discussed here [17].

Oxide-based electrochromics came into the limelight during the first half of the 1980s, when it became widely accepted that this technology can be of great significance for *energy-efficient fenestration* [18, 19]. The term 'smart' window (alternatively 'intelligent' or 'switching' window) was coined in 1984/1985 [20, 21] and got immediate attention from researchers as well as from media and the general public.

Electrochromic *eyewear* has attracted interest on and off for decades. Photochromic glass or plastic has been widely used in sunglasses and goggles, but photochromic devices have clear limitations: their coloration relies on ultraviolet solar irradiation, so they are not of much use inside buildings and vehicles, and the coloration and bleaching dynamics are undesirably slow especially for bleaching at low temperatures. Electrochromic-based eyewear does not have these drawbacks, which motivates a lingering interest. Studies have been reported for sun goggles [22] and helmet visors [23].

A different type of application regards electrochromic-controlled thermal emittance for *thermal control of spacecraft*. Their exposure to cold space or solar irradiation can yield temperature differences between −50 and +100 °C, which may lead to unreliability in electronic components, detectors and so on. Mechanical shutters can be used for emittance control but tend to be impractical. Investigations on electrochromic-based thermal management have been conducted at least since the early 1990s and remain active today [24–26]. Related devices can be employed for military camouflage in the infrared [27].

The aforementioned applications are not the only ones of interest for electrochromic devices, but the possibility of achieving colour-changing systems based on inorganic oxides or organic materials seems to serve as a catalyst for human inventiveness, and recently mentioned potential uses for electrochromics include fingerprint enhancement in authentication devices and forensics [28] as well as fashion spandex (Lycra — a polyurethane–polyurea copolymer) [29].

1.3 Overview of Electrochromic Oxides

Electrochromic materials and associated devices have been researched continuously ever since the discovery of electrochromism. Looking specifically at electrochromic metal oxides, the literature up to 2007 has been covered in some detail in several prior publications [1, 30–33], and it was noted that some 50–100

scientific and technical papers were published per year. Section 1.3.1 gives a rather superficial presentation of work on electrochromic oxide films presented from 2007. From the sheer number of publications, one may conclude that the research field is thriving and that a large amount of work is devoted to materials based on oxides of W and Ni, as has been the case for the last two decades. Section 1.3.2 discusses optical and electronic properties in electrochromic oxides from a general perspective, and Section 1.3.3 treats these properties in detail for the most widely used electrochromic material, that is, W oxide. Section 1.3.4 discusses ion conduction in electrochromic oxides, again with focus on W oxide. The composition of the electrochromic oxides and their deposition parameters are very important, and some examples from recent studies are given in Section 1.3.5. Finally, Section 1.3.6 reports data on electrochromic properties for films in the full compositional range of W–Ni oxide.

It should be pointed out that much can be inferred about the electrochromic oxides also from studies on alternative applications such as gas sensors and gasochromics, electrical batteries, photocatalysts and so on [34], so the actual knowledge basis for the electrochromic oxides is much larger than the one outlined in this chapter.

1.3.1
Recent Work on Electrochromic Oxide Thin Films

There are two principally different kinds of electrochromic oxides: 'cathodic' ones colouring under ion insertion and 'anodic' ones colouring under ion extraction. Figure 1.2 indicates metals capable of forming oxides of these two categories and also points out that oxides based on vanadium are intermediate [1]. This scheme serves as a natural starting point for a survey of the recent scientific literature on electrochromic oxides. In the following, we first treat the cathodic oxides, then the anodic oxides and finally the intermediate one.

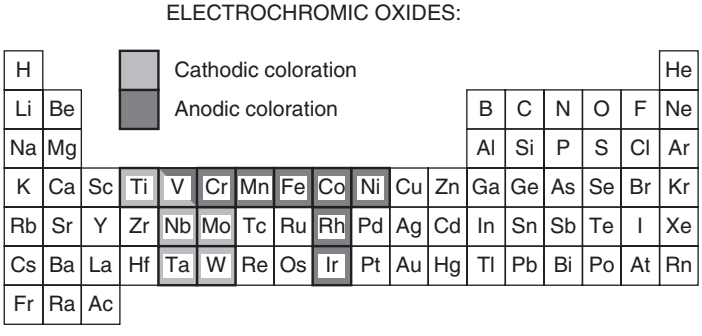

Figure 1.2 Periodic system of the elements (except the lanthanides and actinides). Differently shaded boxes indicate transition metals with oxides capable of giving cathodic and anodic electrochromism. From Ref. [1].

Tungsten oxide remains the most widely studied electrochromic oxide, and films of this *cathodically colouring* material have been prepared by a huge number of techniques, including traditional thin-film preparation with physical and chemical vapour deposition, a plethora of chemical methods, electrochemical methods and others. Surveys of these techniques can be found in a number of books and review papers [35–40]. Nanoparticles have sometimes been used as intermediate steps for the films, and substrate templating has been employed to improve the electrochromic performance.

Regarding physical vapour deposition, data have been reported on W oxide films prepared by thermal evaporation, sputtering and pulsed laser deposition. Other work has used chemical vapour deposition and related spray pyrolysis, and a large number of investigations have been based on chemical routes for making films. Furthermore, electrodeposition, anodisation and electrophoretic deposition have been employed. A useful review has been published on properties, synthesis and applications of nanostructured W oxide [41].

Mixed oxides based on tungsten can exhibit properties that are superior, in one way or another, to those of the pure oxide. One well-studied option is W–Ti oxide, where the addition of titanium leads to significantly enhanced durability under electrochemical cycling, as has been known for many years [42, 43]. Recent work on electrochromism of W–Ti oxide has been reported for films made by sputtering, spray pyrolysis, chemical techniques, electrodeposition and anodisation. A key result is that addition of Ti stabilises a highly disordered structure [44, 45], as also reported in other work on W–Ti oxide that was not specifically on electrochromism [46]. Additional research on mixed oxides has been carried out on films of W–M_W oxide with M_W being Li, C, N, V, Ni, Nb, Mo, Ru, Sn and Ta. Furthermore, investigations have been reported on W oxide containing coinage metal nanoparticles capable of giving plasmon-induced optical absorption of visible light, specifically for nanoparticles of Ag, Pt and Au; using, instead, nanoparticles of indium-tin oxide (ITO) makes it possible to have plasmon absorption at infrared wavelengths. Finally, a number of hybrid nanomaterials have been studied, such as WO_3–PEDOT:PSS, where the second component is poly(3,4-ethylenedioxythiophene):poly(styrenesulfonate).

Electrochromic Mo oxide has many similarities to W oxide, and studies have been performed on films prepared by evaporation, chemical vapour deposition, wet chemical techniques and electrodeposition. Mixed oxides have been researched for Mo–M_{Mo} oxide with M_{Mo} being C, Ti, V, Nb and Ce.

Concerning Ti oxide, electrochromic properties have been reported for films made by sputtering, chemical vapour deposition and spray pyrolysis, various wet chemical techniques, doctor blading and anodisation. This oxide has also been used as anchoring agent for organic chromophores (such as viologens, see Chapter 3) and for inorganic compounds (such as 'Prussian Blue', see Chapter 2). Work has been published for films of Ti–M_{Ti} with M_{Ti} being V and Zr. Finally, studies have been reported on electrochromism of Nb oxide and Nb–Mo oxide.

Regarding *anodically colouring* electrochromic oxides, we first note work on Ir oxide prepared by sputter deposition and by sol–gel technology, and

Ir–Sn oxide prepared by evaporation and Ir–Ta oxide by sputtering. However, iridium oxide is too expensive for most applications, even if diluted with less costly Sn or Ta. Ni oxide is a good alternative whose electrochromic activity was discovered many years ago, and Ni-oxide-based films are included in several of today's electrochromic devices. Recent work has been reported on Ni oxide films prepared by thermal evaporation, sputter deposition, chemical vapour deposition and spray pyrolysis, various chemical techniques and electrodeposition. Furthermore, Ni oxide pigments have been deposited from water dispersion. Mixed binary oxides of Ni–M_{Ni} have been studied for M_{Ni} being Li, C, N, F, Al, Ti, V, Mn, Co, Cu and W. One reason why additions to Ni oxide are of interest is that the luminous transmittance can be enhanced [47]. Further improvements are possible with ternary or more complex oxides with M_{Ni} being (Li,W) [48], (Li,Al) [49], (Li,Zr) [50] and LiPON [51]. Films of the latter materials were produced recently by sputter deposition and are of particular interest for practical applications in future electrochromic-based fenestration. Hybrid films have been made of Ni oxide and one of several polymers or graphene oxide.

V-pentoxide-based films with *intermediate* electrochromic properties have been prepared by vacuum evaporation, sputter deposition, spray pyrolysis, chemical techniques, electrodeposition and inkjet printing. Mixed oxides based on V–M_V have been investigated with M_V being C, Na, Ti, Mo, Ag, Ta and W. Mixed V–Ti oxides can serve as good counter electrodes in electrochromic devices [52, 53].

1.3.2
Optical and Electronic Effects

Most oxide-based electrochromic devices employ two electrochromic films, and it is clearly advantageous to combine one cathodic oxide (e.g. based on W, Mo, Ti or Nb) and another anodic oxide (e.g. based on Ni or Ir). Applying a voltage in order to transport ions and electrons between the two electrochromic films in one direction makes both of these films colour, and transporting ions and electrons in the other direction makes both of them bleach. By combining cathodic and anodic oxides, one can accomplish a rather neutral visual appearance. The most commonly used oxides are based on tungsten and nickel, which exhibit cathodic and anodic electrochromism, respectively, according to the highly schematic reactions [1]

$$[WO_3 + H^+ + e^-]_{\text{bleached}} \leftrightarrow [HWO_3]_{\text{coloured}} \tag{1.1}$$

and

$$[Ni(OH)_2]_{\text{bleached}} \leftrightarrow [NiOOH + H^+ + e^-]_{\text{coloured}} \tag{1.2}$$

for the case of proton insertion/extraction. Electrons are denoted e^-.

We now consider the origin of the electrochromic properties in these oxides and first look at their crystalline nature. The pertinent structures fall into three categories: (defect) perovskites, rutiles and layer/block configurations.

These structures can be treated within a unified framework with 'ubiquitous' MO_6 octahedra (where M denotes metal) connected via joint corners and/or joint edges [1, 54]. Edge-sharing is associated with some degree of octahedral deformation. Only two oxides are problematical within this description: the first one is vanadium pentoxide (V_2O_5), whose crystal structure can be constructed from heavily distorted VO_6 octahedra or, alternatively, from square pyramidal VO_5 units [55, 56]; and the second example is hydrous nickel oxide – which is the actual electrochromic material rather than pure NiO [57, 58] – which is thought to contain layers of edge-sharing NiO_6 octahedra.

Octahedral coordination is essential for the electronic properties of electrochromic oxides [1, 54]. It was shown in detail many years ago [59] that oxygen *2p* bands are separated from metal *d* levels, and octahedral symmetry leads to splitting of these latter levels into bands with the conventional designations e_g and t_{2g}. Figure 1.3 illustrates three cases of importance for the electrochromic oxides. Left-hand panel, for H_xWO_3, indicates that the O*2p* band is separated from the split *d* band by an energy gap. Pure WO_3 has a full O*2p* band and an empty *d* band, and the band gap is wide enough to render films of this material transparent. Inserting small ions and charge-balancing electrons – according to the aforementioned 'battery' model – leads to a partial filling of the *d* band along with optical absorption as discussed later. The middle panel in Figure 1.3 is adequate for anodically colouring electrochromic oxides. The pure oxides have unoccupied t_{2g} states, and insertion of ions and electrons may fill these states to the top of the band, so the material exhibits a gap between the e_g and t_{2g} levels. The material then becomes transparent, assuming that the band gap is large enough. Finally, the right-hand part of Figure 1.3 indicates that V_2O_5 – with both cathodic and anodic features in its electrochromism – has a principally

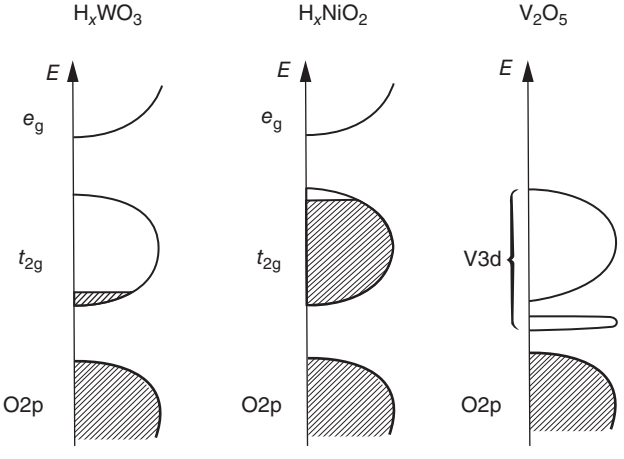

Figure 1.3 Schematic band structures for different types of electrochromic oxides, as discussed in the main text. Shaded regions signify filled states and *E* denotes energy. From Ref. [1].

different electronic structure. The deviation from octahedral coordination is significant enough that the *d* band displays a narrow split-off part in the band gap. Insertion of ions and electrons into V_2O_5 may fill this narrow band so that the optical band gap is widened. These features of the band structure can account for electrochromism of V_2O_5 [60], at least in principle, as well as band gap widening during photo-injection of hydrogen into this material [61].

The detailed mechanism for optical absorption in the electrochromic oxides is often poorly understood. The exception may be W oxide, which is considered in the following section, whose properties were reviewed some years ago [33]. However, optical absorption in electrochromic oxides is generally believed to be connected with charge transfer, and polaron absorption accounts for at least most of the significant features [33, 62–65]. A simplified, but closely related, model for the absorption considers intervalence charge transfer transitions [66].

1.3.3
Charge Transfer Absorption in Tungsten Oxide

Electrons inserted together with ions are localised on metal ions and, for the case of tungsten oxide, change some of the W^{6+} sites to W^{5+}. Charge transfer between sites *i* and *j* can be expressed, schematically, as

$$W_i^{5+} + W_j^{6+} + \text{photon} \rightarrow W_i^{6+} + W_j^{5+} \tag{1.3}$$

More specifically, the electrons are thought to enter localised states positioned 0.1–0.2 eV below the conduction band and displace the atoms surrounding them so that they form a potential well; strong electron–phonon interaction then leads to the creation of small polarons with a size of 0.5–0.6 nm [33].

Figure 1.4, taken from the work of Berggren *et al.* [65], reports data on the optical absorption coefficient of sputter-deposited W oxide films electrochemically intercalated with Li^+ ions to a number of different levels *x* (defined as the number of Li^+ ions per W atom). It is found that Li^+ intercalation yields a broad and asymmetric peak at an energy of ~1.3 eV. For large intercalation levels, this peak is shifted slightly towards higher energies.

Figure 1.5 shows data from a comparison of the spectral absorption coefficient at two intercalation levels with Bryksin's theory of polaron absorption [63], which is based on intraband transitions between localised energy levels in a Gaussian density of states [65]. Theory and experiments are found to agree well both for $x = 0.04$ and $x = 0.36$, as seen from Figure 1.5(a) and (b), respectively. A comparison with the more recent theory by He [64] does show equally good correspondence, especially not at low intercalation. Successful comparison between Bryksin's theory and experimental optical data was presented several years ago also in other work on W oxide films [67], and further data on polaron absorption in the same material have been given recently [68].

The simple model for charge exchange, outlined earlier, is credible only as long as transitions can take place from a state occupied by an electron to another state capable of receiving the electron. If the ion and electron insertion levels are large,

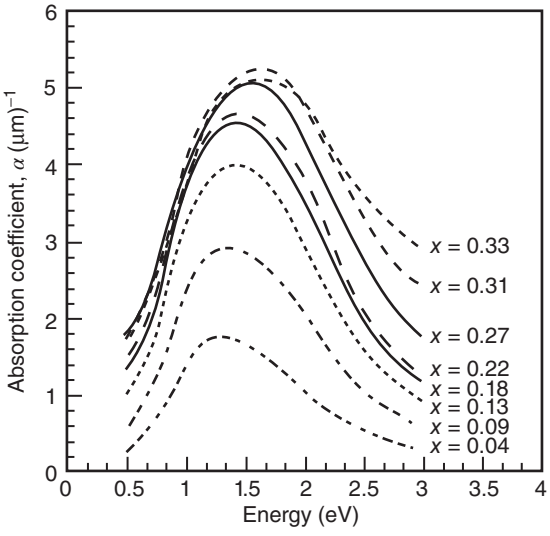

Figure 1.4 Spectral absorption coefficient for W oxide films with different intercalation levels, where x denotes the Li^+/W ratio. From Ref. [65].

this assumption is no longer the case and then 'site saturation' [69] becomes important, as considered next.

A detailed investigation of the optical properties at different amounts of lithium insertion into sputter-deposited W oxide films was reported recently by Berggren and Niklasson [70] and Berggren *et al.* [71], and data are available also for hydrogen-containing material [72]. Figure 1.6a reports spectral optical absorption coefficient α for different levels of Li^+ intercalation into a W oxide film. A broad absorption band evolves at an energy of ~1.5 eV for low values of x, as also observed earlier, while the absorption peak shifts towards higher energies for large amounts of Li. The strong increase of α above 3.5 eV is associated with the fundamental band gap of W oxide. It is interesting to subtract the absorption due to the unintercalated material, and the corresponding absorption coefficients, denoted α^+, are given in Figure 1.6b which indicates that the data have unambiguous peak structures. The data could be modelled with three Gaussian peaks, whereas modelling with only two peaks was unsuccessful. Two of the peaks were at the positions shown in Figure 1.6b, and the third peak could be located at intermediate energies. Figure 1.7 indicates the integrated strengths of these peaks.

The origin of the Gaussian peaks can be reconciled with 'site saturation' by considering three types of sites, namely W^{4+}, W^{5+} and W^{6+}. Beginning with empty states ($x = 0$), most of the states will be singly occupied at the start of the intercalation, and electron transitions between empty and singly occupied states will be prevalent. As more single states are filled, the probability that doubly occupied states also will be formed will be higher. Analytical expressions for the number of possible electronic transitions can be given for $W^{6+} \leftrightarrow W^{5+}$, $W^{5+} \leftrightarrow W^{4+}$ and

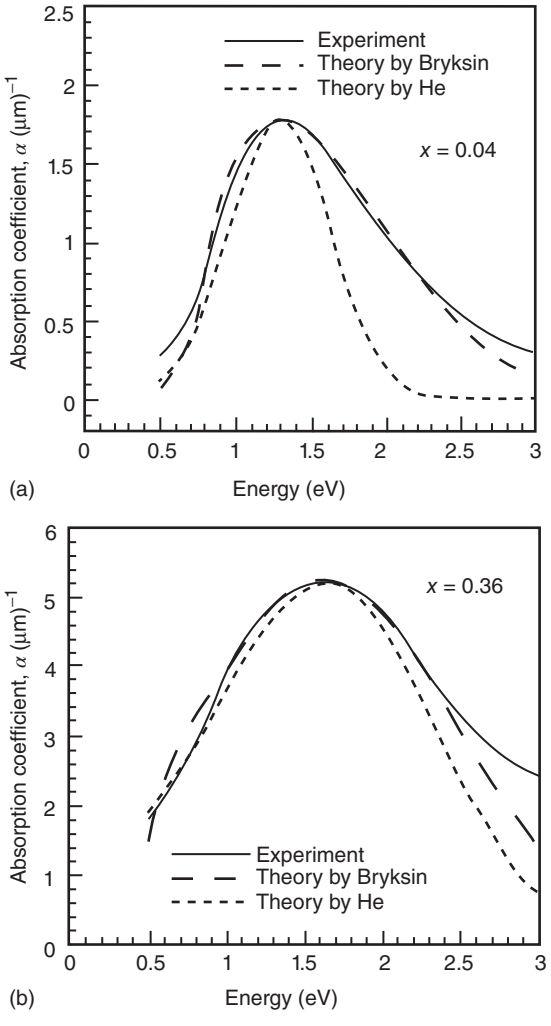

Figure 1.5 Spectral absorption as measured (cf. Figure 1.4) and calculated from two theories of polaron absorption at two intercalation levels, where x denotes Li^+/W ratio. From Ref. [65].

$W^{6+} \leftrightarrow W^{4+}$ by $2x(2-x)^3$, $2x^3(2-x)$ and $x^2(2-x)^2$, respectively [71]. Corresponding curves are given in Figure 1.8, and it is clear that there is good similarity with the integrated peak structure in Figure 1.7, which hence indicates that 'site saturation' takes place. The intensities of the curves do not coincide, which is not surprising since the absorption strength per transition is likely to be different for the three cases. Considering a practical electrochromic device, long-term cycling durability demands that x is kept low, perhaps not exceeding 0.3–0.35, and then the $W^{5+} \leftrightarrow W^{6+}$ transitions are clearly dominating.

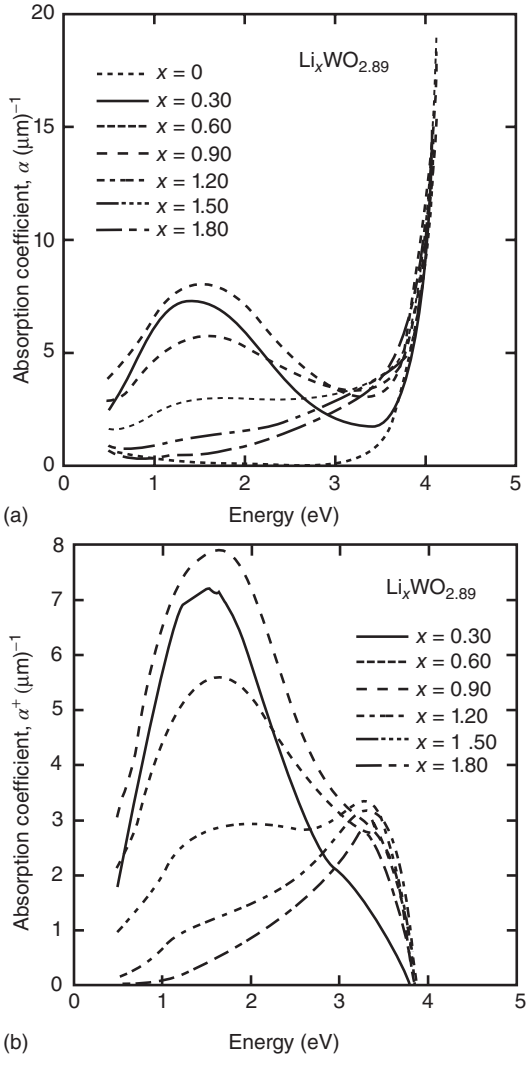

Figure 1.6 Panel (a) shows spectral absorption coefficient α for a slightly sub-stoichiometric W oxide film intercalated to the shown Li^+/W ratios *x*, and panel (b) shows corresponding absorption α^+ when the absorption of the unintercalated film in panel (a) has been subtracted. From Ref. [71].

1.3.4
Ionic Effects

Most electrochromic oxides consist of octahedral units in various arrangements, as discussed in detail in Section 1.3.2. These oxides are appropriate both because of their electronic features and because the spaces between the octahedral units

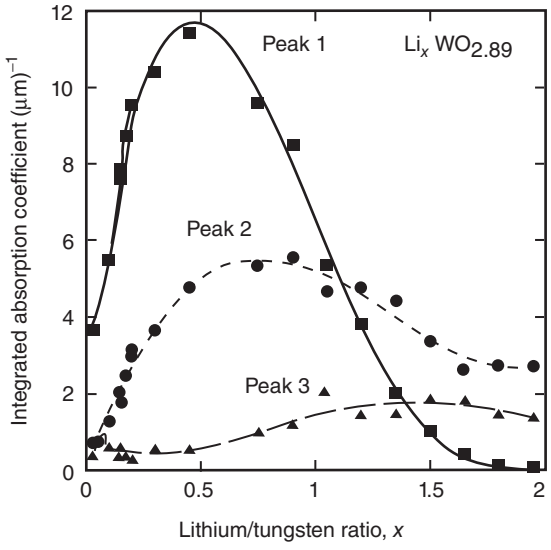

Figure 1.7 Integrated absorption coefficient as a function of Li^+/W ratio x for three Gaussian peaks representing the data in Figure 1.6b. From Ref. [71].

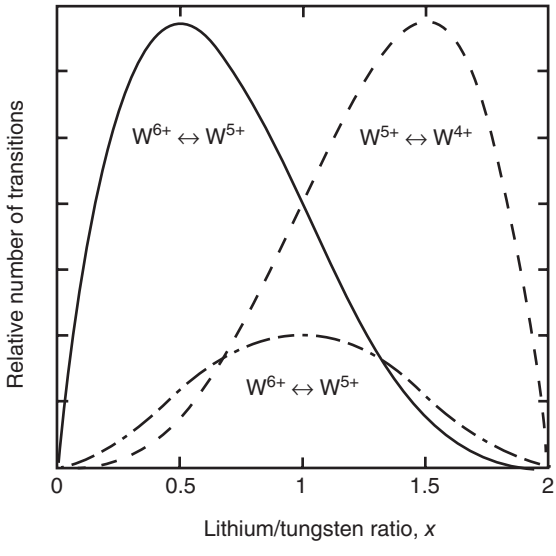

Figure 1.8 Relative number of transitions of the types $W^{6+} \leftrightarrow W^{5+}$, $W^{5+} \leftrightarrow W^{4+}$ and $W^{6+} \leftrightarrow W^{4+}$ as a function of Li^+/W ratio x. From Ref. [71].

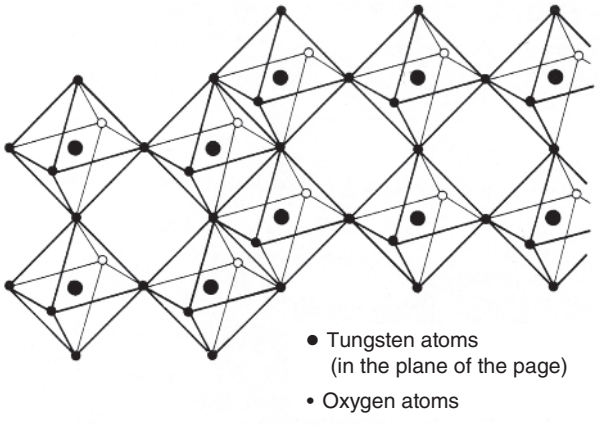

Figure 1.9 Schematic image of corner-sharing and edge-sharing octahedra in slightly sub-stoichiometric crystalline W oxide. From Ref. [1].

are sufficiently large to allow facile transport of small ions. Clusters of octahedra are able to form disordered and more or less loosely packed aggregates with large porosity, and it follows that nanostructures enter at two or more length scales. The following discussion is again focused on W oxide, which has been investigated in great detail. It is not obvious that the anodic electrochromic oxides can be understood on the same premises however, and grain boundaries may then be of large significance, but the situation remains unclear.

Figure 1.9 illustrates nanostructural features of W oxide and shows WO_6 octahedra, each with six oxygen atoms surrounding a tungsten atom. Stoichiometric WO_3 has a structure wherein each octahedron shares corners with neighbouring octahedra. WO_3 and similar transition-metal-based oxides easily form sub-stoichiometric oxides, which include a certain amount of edge-sharing octahedra. The three-dimensional structure comprised by the octahedra yields a three-dimensional 'tunnels' structure conducive for ion transport.

The crystalline structure in Figure 1.9 is simplified and refers to a cubic structure (cf. Figure 1.10a), and a tetragonal structure usually prevails in WO_3 at normal temperature and pressure. The tetragonal structure is more favourable for ion transport than the cubic one since the separations among the octahedral units are larger, as shown in Figure 1.10b. Hexagonal structures, indicated in Figure 1.10c, are easily formed in thin films [1, 73, 74] of W oxide, and the structure is then even better suited for the transport of ions.

Figure 1.11 indicates structural data based on modelling of X-ray scattering from films made by evaporation onto substrates at different temperatures, from room temperature to 300 °C [75]. Cluster-type structures are apparent and include hexagonal-type units, which grow in size and interconnect at high substrate temperatures.

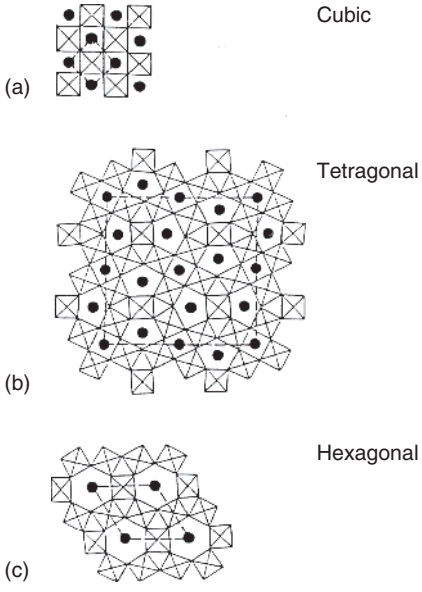

Figure 1.10 W oxide with cubic (a), tetragonal (b) and hexagonal (c) structure. Dots signify sites for ion insertion in spaces between the WO_6 octahedra. Dashed lines show extents of the unit cells. From Ref. [1].

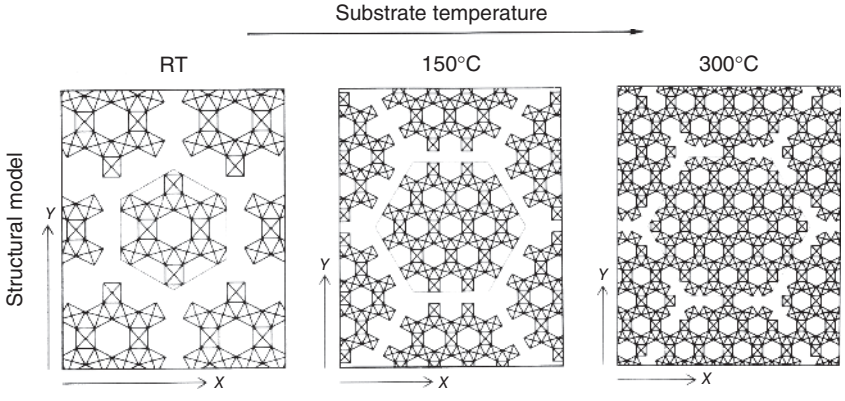

Figure 1.11 Structural models for WO_6 octahedra in W oxide films prepared by evaporation onto substrates at the shown temperatures (RT denotes room temperature). Arrows in the *x* and *y* directions are 2 nm in length. After Ref. [75].

Larger nanostructures than those created by the aggregation of octahedral units can occur as a consequence of the limited mobility of the deposition species, and this mechanism is important for thin films prepared by most techniques. Regarding sputter deposition, the main features are captured in a 'zone diagram', commonly referred to as a 'Thornton diagram' [76]. It is shown in Figure 1.12. More elaborated or specialised versions of this diagram have been presented in subsequent work. It is evident that low substrate temperature and high pressure in the sputter plasma lead to nanoporous features appropriate for

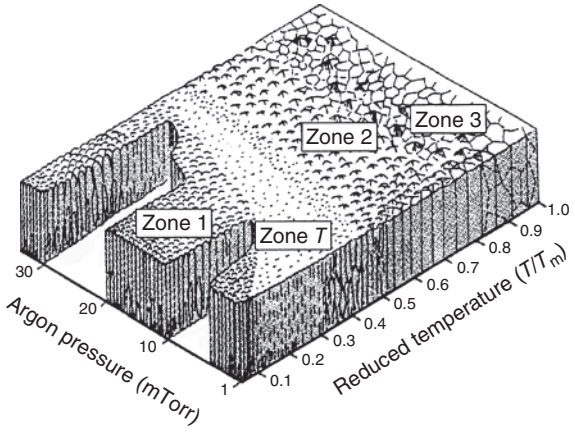

Figure 1.12 Schematic nanostructures in sputter-deposited thin films formed at different pressures in the sputter plasma and at different substrate temperatures. The melting temperature of the material is denoted T_m. From Ref. [76].

ion transport across the film thickness and hence for electrochromic devices. A direct correlation between sputter gas pressure and electrochromic performance was reported recently [77]. Oblique angle deposition can promote porosity still further, as specifically shown for W-oxide-based films [78–80]. Annealing (cf. Figure 1.11) and ion irradiation [81] are other ways to influence film density.

W oxide films can involve molecular deposition species, and it is of interest to consider the lowest energy structures of $(WO_3)_q$ clusters, which may form the deformable building blocks for octahedra-based nanostructures. Such clusters were evaluated from first-principle calculations in recent work by Sai *et al.* [82]. Data for $2 \leq q \leq 12$ are depicted in Figure 1.13, from which it can be inferred that small clusters (with q equal to 3 and 4) have ring-like configurations with alternating W–O arrangements, while larger clusters (with $q \geq 8$) can be described as symmetric spherical-like cages. Trimeric W_3O_9 molecules form during evaporation [83] and correspond to $q = 3$ in the cluster model; these structures are characterised by a hexagonal configuration. Aqueous solutions, useful for liquid-phase film deposition, can have a preponderance of $(W_6O_{19})^{2-}$ ions, known as 'Lindqvist anions' [84].

1.3.5
On the Importance of Thin-Film Deposition Parameters

Irrespective of the technique for making EC thin films, the detailed deposition conditions usually play a decisive role. However, each technique is unique to a considerable extent and little can be said in general apart from the guidelines inferred from the previous section.

We first look at films made by physical vapour deposition, which is notable for its possibilities to accomplish process control and reproducibility. A clear

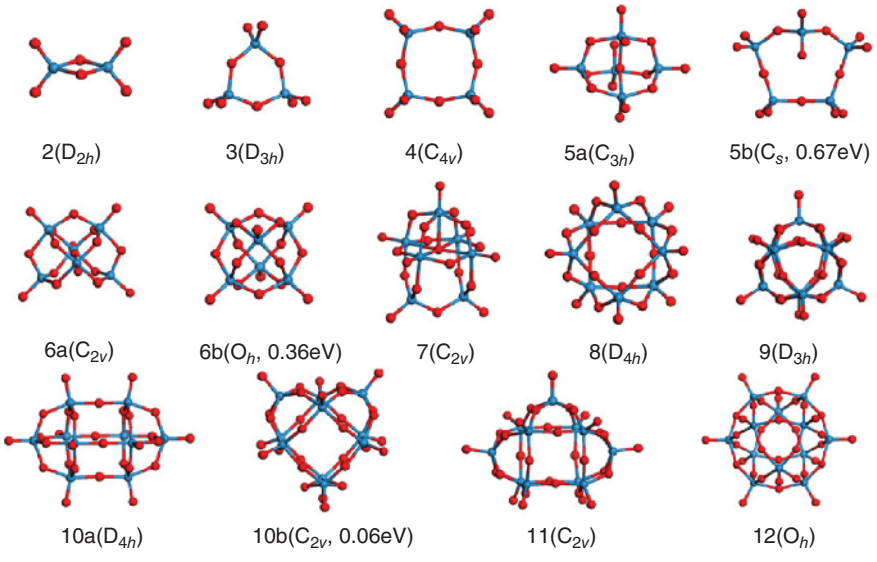

Figure 1.13 Lowest-energy structures of $(WO_3)_q$ clusters with $2 \leq q \leq 12$ and metastable isomers (denoted 5b, 6b and 10b). Crystallographic symmetry designations are indicated at the various clusters. From Ref. [82].

illustration of the applicability of the Thornton diagram in Figure 1.12 for electrochromic films was found in recent work on titanium-oxide-based films made by sputtering at various pressures p onto substrates at different temperatures τ_s [85, 86]. Figure 1.14, reproduced from work by Sorar *et al.* [85], shows cyclic voltammograms indicating current density under charge insertion and extraction as a function of applied voltage. Clearly, $p > 10$ mTorr and $\tau_s < 100\,^{\circ}\mathrm{C}$ are required to accomplish a structure porous enough for facile ion transport.

The composition of the sputter gas is very important, in addition to its pressure, as elucidated in Figure 1.15 for water vapour added to $Ar + O_2$ during sputter deposition of Ni oxide films; the results were presented recently by Green *et al.* [87]. Addition of water vapour to a pressure of $\sim 7 \times 10^{-2}$ Pa increased the current density during ion insertion and extraction and enlarged the optical modulation by allowing a darker state. Other work on sputtering of Ni oxide in the presence of water vapour has been reported elsewhere [88, 89].

The properties of the substrate for the electrochromic film may be of large significance. One example of this dependence is reported in Figure 1.16a, taken from work by Yuan *et al.* [90], which shows optical transmittance in bleached and coloured states for a Ni oxide film prepared by electrodeposition onto a substrate with and without a layer of self-assembled polystyrene nanospheres. Clearly, the sphere templating yields a lower coloured-state transmittance. The visual appearance of films on untreated and templated substrates is shown in Figure 1.16b.

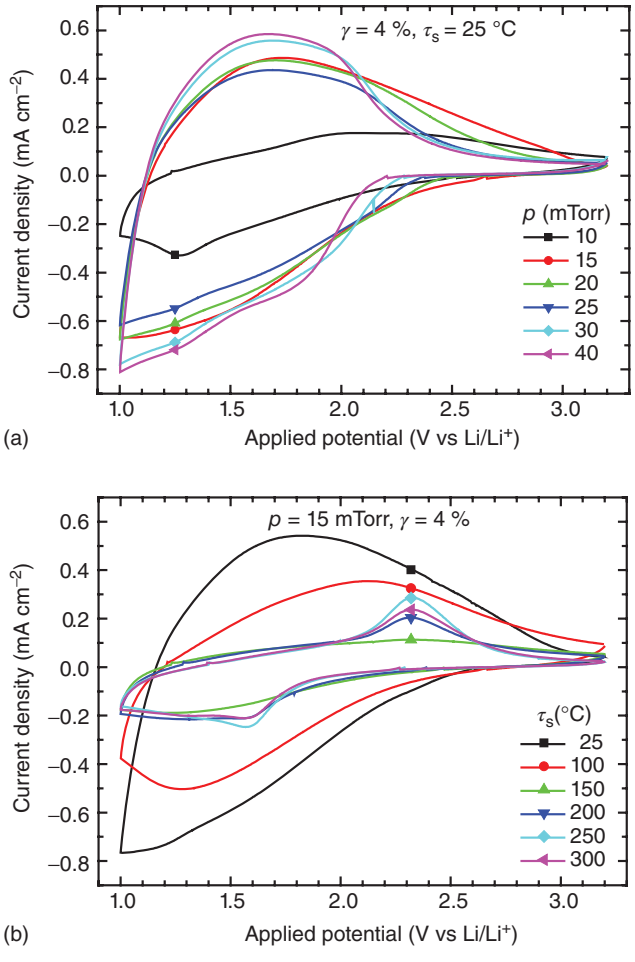

Figure 1.14 Cyclic voltammograms for sputter-deposited TiO_2-based film in a Li^+-conducting electrolyte. Film deposition took place at the pressure p and oxygen/argon ratio γ onto substrates at temperature τ_s. Data in panels (a) and (b) refer to the effects of varying p and τ_s, respectively. From Ref. [85].

The deposition rate is a very important parameter, which often more or less determines the cost for industrial coating production. However, this parameter is not commonly reported in scientific papers. Among high-rate techniques, it is particularly interesting to consider reactive-gas-flow sputtering, which was studied recently by Oka *et al.* [91] to make W oxide films. Figure 1.17 shows deposition rate, oxygen/tungsten stoichiometry and density for films made by sputtering at two different oxygen flows but under otherwise identical conditions. The deposition rate was found to be as high as $\sim 4\,nm\,s^{-1}$, which is considerably higher than for typical reactive DC magnetron sputtering. The density depended on the oxygen gas flow and could be as low as half of the bulk value for WO_3 ($7.16\,g\,cm^{-3}$).

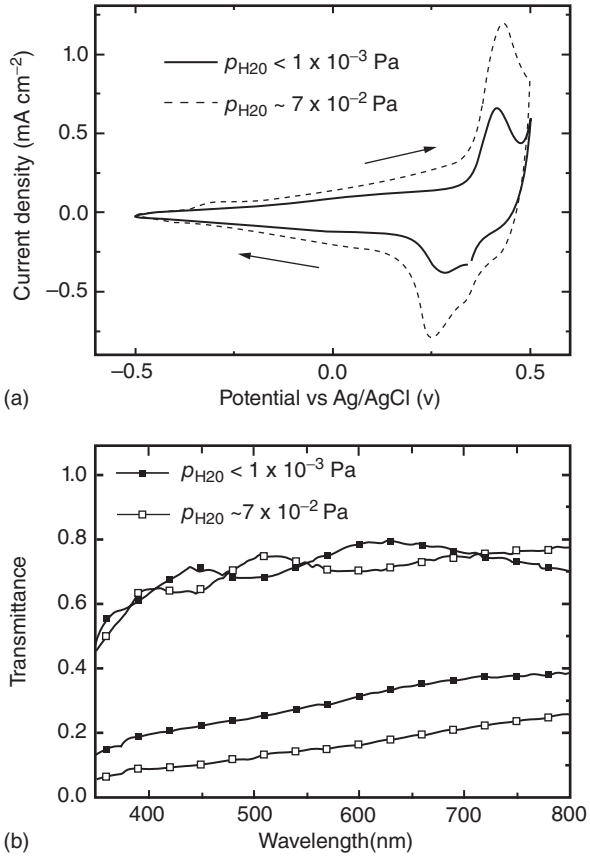

Figure 1.15 Current density during ion insertion/extraction (a) and spectral transmittance at maximum and minimum intercalation (b) for sputter-deposited Ni oxide films prepared with the shown partial pressures of H_2O in the sputter gas. From Ref. [87].

Hence, the film structure is highly porous and suited for electrochromic devices. Not surprisingly, investigations of the electrochromic performance showed good results. Another contemporary high-rate deposition technique, appropriate for W oxide, is high-power impulse magnetron sputtering (known as HiPIMS) [92].

1.3.6
Electrochromism in Films of Mixed Oxide: The W–Ni-Oxide System

Electrochromism has been investigated in many binary, ternary and so on, oxides, as surveyed in Section 1.3.1. Nevertheless, there is a general lack of comprehensive investigations across the full compositional range between the component oxides. An exception is the W–Ni oxide system, denoted Ni_xW_{1-x} oxide, which was studied by Green *et al.* [93–98] and clearly combines cathodically and anodically colouring oxides. Tungsten-rich sputter-deposited films were found to

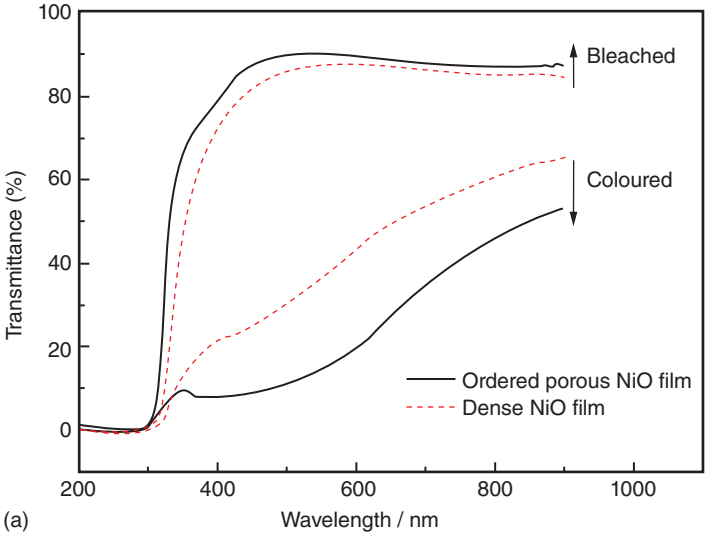

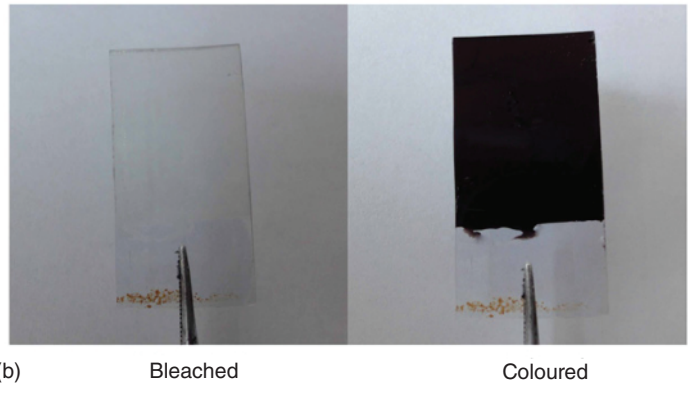

Figure 1.16 Spectral transmittance (a) and visual appearance (b) of an electroplated Ni oxide film on a substrate with and without a template layer consisting of polystyrene nanospheres. The film is in its fully coloured and bleached states. From Ref. [90].

consist of a mixture of amorphous WO_3 and nanocrystalline $NiWO_4$, with equal amounts of W and Ni the structure was dominated by $NiWO_4$, and nickel-rich films were made up of nanocrystalline NiO and $NiWO_4$.

Figure 1.18 shows optical absorption coefficients at a mid-luminous wavelength of 550 nm for fully coloured and bleached films. The electrochromism is seen to be much stronger in W oxide than in Ni oxide. For W-rich films, the absorption coefficient drops as Ni fraction x is increased, except at the composition $x \approx 0.12$ where a pronounced peak can be seen in the absorption coefficient. For Ni-rich films, the absorption coefficient rises as x approaches unity. Films in the compositional range $0.3 < x < 0.7$ do not display electrochromism. Another important parameter

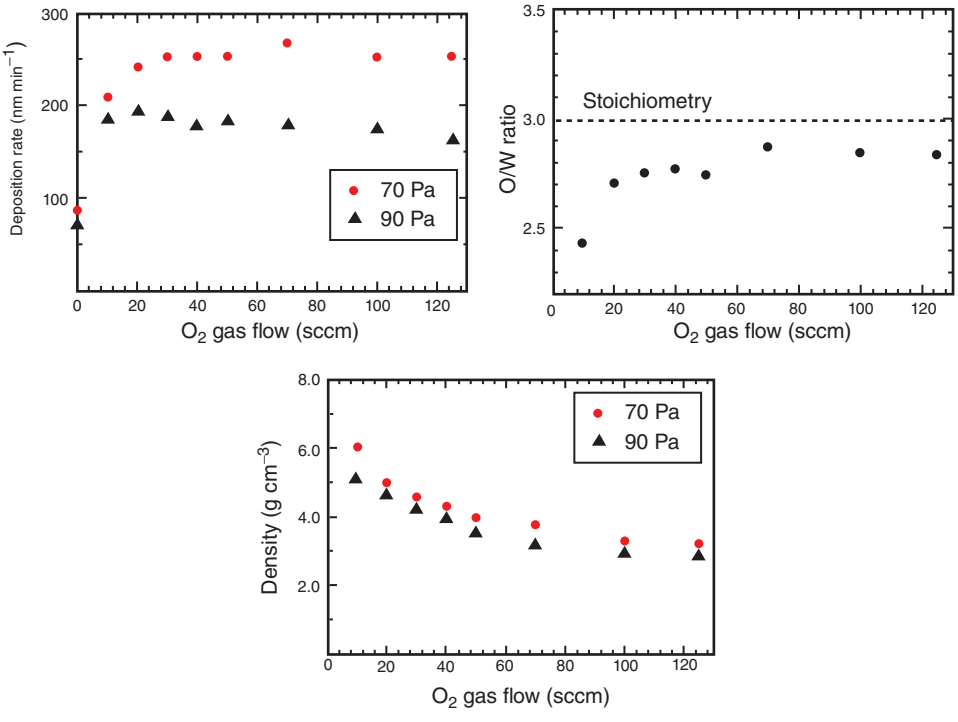

Figure 1.17 Deposition rate, oxygen/tungsten stoichiometry and density of thin films of electrochromic W oxide prepared by reactive-gas-flow sputtering at different oxygen gas flows. The total gas pressure was 70 Pa, and for two of the data sets also 90 Pa. From Ref. [91].

for electrochromic films is coloration efficiency η, defined by $\eta = \mathrm{OD}/\Delta Q$ where optical density (OD) is absorption coefficient multiplied by film thickness and ΔQ is inserted/extracted charge density. Figure 1.19 shows data on coloration efficiency and allows easy comparison with Figure 1.18. Obviously, η increases slightly for increasing values of x, except for compositions around $x \approx 0.5$ where η is approximately zero.

The strong optical absorption at $x \approx 0.12$ is interesting for electrochromic device applications, and Figure 1.20 reports spectral coloration efficiency for films of pure W oxide and for Ni_xW_{1-x} oxide films with two values of x. It is evident that good performance of films with $x \approx 0.12$ is found in the whole luminous wavelength range, that is, for 400–700 nm.

1.4
Transparent Electrical Conductors and Electrolytes

An electrochromic device does not only include electrochromic thin films but also incorporates transparent electrical conductors and an electrolyte, as seen

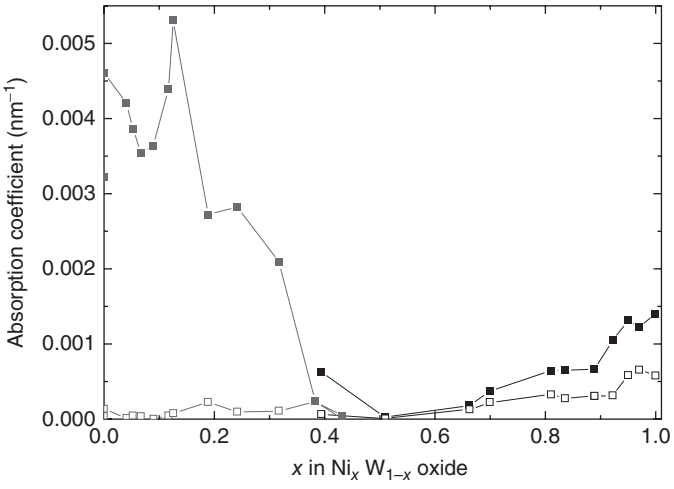

Figure 1.18 Mid-luminous absorption coefficient as a function of composition for electrochromic thin films of W–Ni oxide. Filled and open symbols denote fully coloured and bleached states, respectively. From Ref. [95].

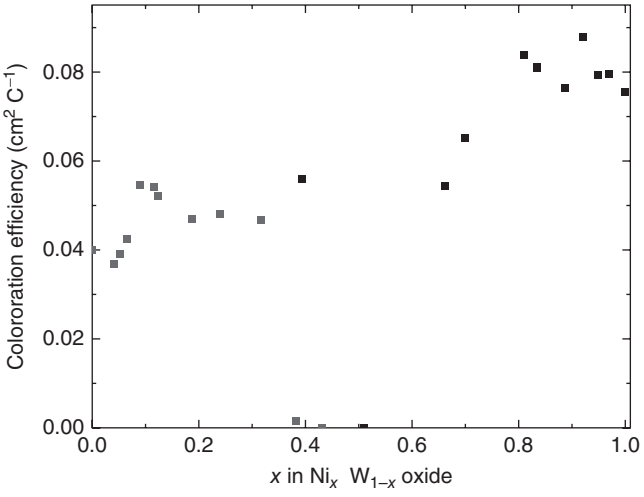

Figure 1.19 Mid-luminous coloration efficiency as a function of composition for electrochromic thin films of W–Ni oxide. From Ref. [95].

in Figure 1.1. The transparent electrical conductors may be the most costly part in the device – especially if they are based on an indium-containing oxide – and clearly deserve attention. They are of critical importance not only in electrochromics but also for thin-film solar cells, light emitting devices and so on. There are several recent reviews covering the field of transparent conductors [32, 99–101], and therefore only a bird's-eye view is given here, though with some

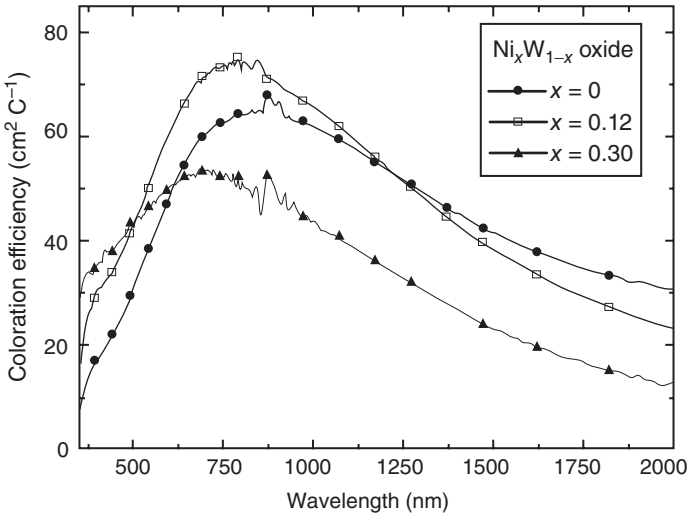

Figure 1.20 Spectral coloration efficiency for W–Ni oxide films with the shown compositions. From Ref. [94].

attention to very recent work and to transparent conductors suitable for flexible substrates. There are several types of transparent conductors with specific pros and cons; semiconductor-based films are treated in Section 1.4.1, metal-based films in Section 1.4.2 and nanowire-based and other alternatives in Section 1.4.3. Electrolytes for electrochromic devices are surveyed in Section 1.4.4 with foci on thin films and polymer layers.

1.4.1
Transparent Electrical Conductors: Oxide Films

Thin films of heavily doped wide-bandgap conducting oxides are commonly used in electrochromic devices. These materials include In_2O_3:Sn (ITO), In_2O_3:Zn, ZnO:Al, ZnO:Ga, ZnO:In, ZnO:Si, ZnO:B, SnO_2:F (FTO), SnO_2:Sb and TiO_2:Nb; their doping levels are typically a few atomic percent. Several of the oxides can combine a resistivity as low as $\sim 1 \times 10^{-4}\,\Omega\,\text{cm}$ with excellent luminous transmittance and durability. Films of ITO, ZnO:Al and ZnO:Ga deposited by reactive DC magnetron sputtering onto glass and PET typically have a resistivity of $\sim 2 \times 10^{-4}$ and $\sim 4 \times 10^{-4}\,\Omega\,\text{cm}$, respectively. High-quality FTO films are normally made by spray pyrolysis in conjunction with float glass production, and high temperatures are necessary also for TiO_2:Nb films. All of these oxides are transparent across most of the solar spectrum, as seen in Figure 1.21 for FTO-coated glass [102]. The oxide-based transparent conductors are very well understood theoretically [103–105], which means that detailed and accurate simulations of optical properties can be made for multilayer configurations such as electrochromic devices.

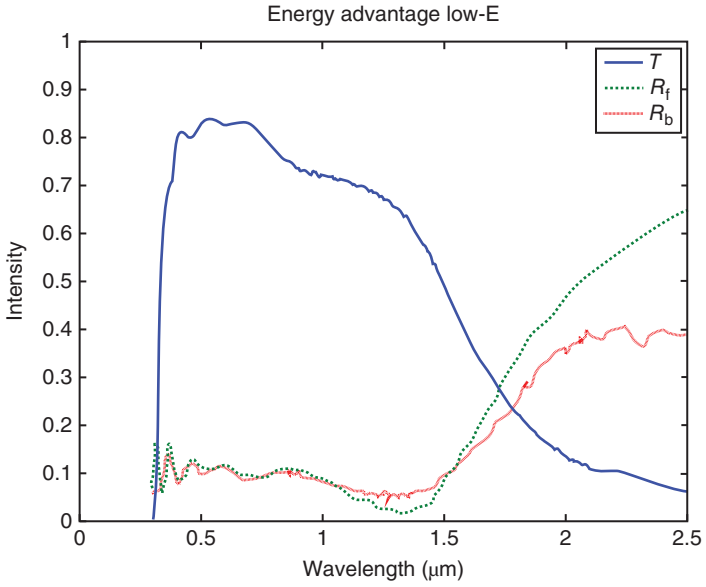

Figure 1.21 Spectral transmittance T and reflectance from the front (coated) side (R_f) and the back side (R_b) for commercial FTO-coated glass. The luminous transmittance is 83% and the solar energy transmittance is 71%. From Ref. [102].

Deposition onto flexible substrates introduces risks for cracking and delamination, and thereby lowered electrical conductivity, if the bending radius is smaller than a few centimetres [106, 107]. In general, the fracture behaviour is dependent on film thickness and bending direction. If needed, several techniques can be used to diminish the propensity for cracking.

ITO films are widely used but expensive, even if indium is not one of the rarer elements in the earth's crust [108], and its deposition requires careful process control. ZnO:Al and ZnO:Ga films can reach similar optical and electrical properties but tend to demand even more stringent process supervision, and good FTO and TiO_2:Nb films must be deposited onto hot glass. Clearly, each type of transparent conducting oxide films presents particular challenges, and there is no 'best' option for electrochromic-based and other devices.

Health aspects of indium-based films require attention, and their preparation can lead to pulmonary disorders [109]. This affliction is named 'indium lung' and obviously is a concern for large-scale production of ITO films and particles.

1.4.2
Transparent Electrical Conductors: Metal-Based Films

Metal-based transparent conductors can show excellent properties and avoid the electronic activation barrier that may exist between, for example, W oxide and ITO [110]. Coinage metals (Cu, Ag and Au) have electrical conductivities around 2

orders of magnitude higher than for the best transparent conducting oxide, which means that they can be thin enough that the luminous absorption is only some per cent. Metal films are stretchable to a much larger degree than oxide-based films.

Metal films to be used in transparent conductors must be extremely thin, which means that their properties are strongly affected by the peculiarities of thin-film growth. When metal is deposited onto a substrate of glass or polymer, the condensate goes through a number of more or less distinct growth stages [111]: tiny metallic nuclei form initially; they grow and create increasingly irregular 'islands'; these 'islands' interconnect and produce a contiguous meandering (percolating) network at a thickness that corresponds to 'large-scale coalescence'; the network is then transformed to a film comprising holes; and finally, a well-defined metallic film may be created. The relevant films have thicknesses of the order of 5–10 nm [112].

Interface reflectance limits the luminous transmittance of the coinage metal film to ~50%, but this transmittance can be radically enhanced if the metal film is positioned between high-refractive-index transparent layers anti-reflecting the metal. This effect is shown in Figure 1.22 for an 8.0-nm-thick Au film and for such a film between 55-nm-thick TiO_2 layers, from the work by Lansåker *et al.* [113]. The anti-reflection increases the transmittance to ~80%. This figure also indicates that computations based on thin-film optics can model the optical properties accurately except in the infrared. The ultrathin Au films were durable enough to be used in electrochromic devices [113]. Many other combinations of materials can be employed as alternatives to the one illustrated here, and transparent conductors based on oxide/metal/oxide are of intense interest not only for energy-related applications but also for transparent and flexible electronics and so on.

Silver-based coatings are used on a massive scale in today's fenestration, and it is possible to devise multilayer structures with a luminous transmittance of 80% and minimum throughput of solar energy (known as a 'solar-control' coating) [114, 115]. These coatings may combine two or more metal films in an advanced construction with more than 10 individual layers. Figure 1.23 shows an example of a commercial coating of this type on glass [102]. The figure allows direct comparison with data for the semiconductor-based coating in Figure 1.21.

1.4.3
Transparent Electrical Conductors: Nanowire-Based Coatings and Other Alternatives

Numerous alternatives to transparent conductors based on thin films of oxides and metals are currently investigated. Carbon-based materials are one of these [116]. We first consider graphite, which consists of loosely bound layers of carbon atoms on a honeycomb lattice. Such layers can create nanoparticles, for example, 60-atom units called 'fullerene molecules' as well as *carbon nanotubes* [117]. Single-wall carbon nanotubes can be several centimetres in length and consist of one layer of carbon atoms rolled into a seamless cylinder with a radius up to a few nanometres. There are two types of such carbon nanotubes, with metallic and semiconducting properties; the two fractions can be separated by several

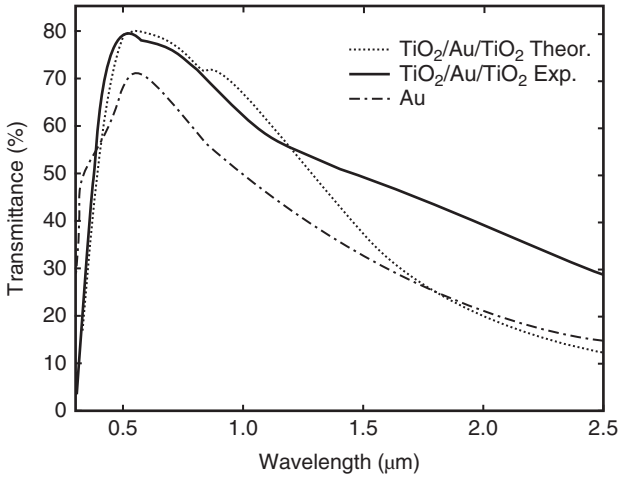

Figure 1.22 Experimental and computed spectral transmittance for Au and TiO_2/Au/TiO_2 films. Film thicknesses were 8 nm for Au and 55 nm for TiO_2. From Ref. [113].

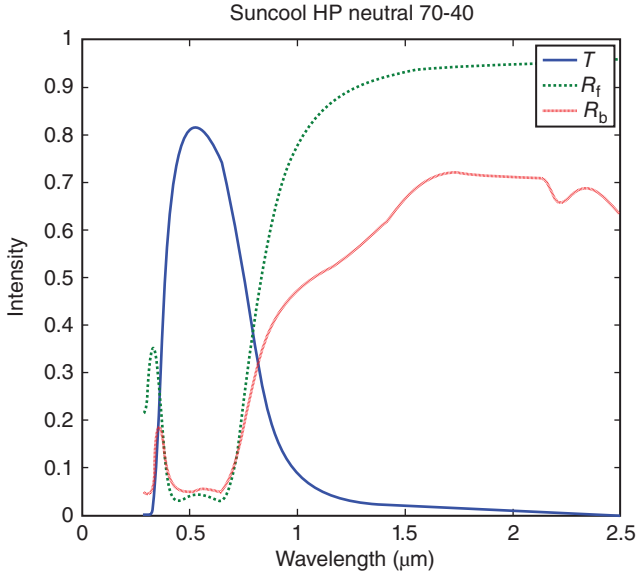

Figure 1.23 Spectral transmittance T and reflectance from the front (coated) side (R_f) and the back side (R_b) for a commercial glass with an Ag-based coating. The luminous transmittance is 80% and the solar energy transmittance is 41%. From Ref. [102].

techniques. Carbon nanotube meshes can be used as transparent conductors and attached to substrates by roll-to-roll coating [118].

Another carbon-based alternative is *graphene,* which consists of atomically thin layers of sp^2-hybridised carbon atoms arranged on a honeycomb lattice [119]. Graphene layers are usually prepared via mechanical or chemical exfoliation of graphite into individual sheets [120] or by chemical vapour deposition [121]; doping can be used to enhance the properties. Roll-to-roll production of graphene coatings have been demonstrated, and up to 30-in.-wide ribbons yielded a sheet resistance as low as ~30 Ω along with ~90% optical transmittance for films comprising four graphene layers [122]. Hot-press lamination onto PET and ink-jet printing are other techniques that can be used for large-area manufacturing.

Meshes of *metal-based nanowires* are another possibility. They can be prepared cheaply by wet-chemical techniques and applied to substrates by 'simple' techniques such as electrospraying and brush painting. A vast amount of research has been performed recently, mainly on silver-based nanowires. The electrical connection between the nanowires can be improved by different techniques such as 'nanowelding' and application of electrical fields. Recent work on metal 'nanotrough' networks demonstrated particularly good optical and electrical properties [123]. It should be noted that nanowire assemblies can have good electrical properties, but the physical dimensions of the individual nanowires make it hard to avoid some diffuse light scattering, as studied recently for silver nanowires [124]. This haze tends to limit applications in electrochromic devices for see-through applications.

Some *organic materials* can be used as transparent conductors, and a good example is poly(3,4-ethylenedioxythiophene) (PEDOT) (see Chapter 5). This material cannot quite compete with the other alternatives with regard to performance but is nevertheless of considerable interest since preparation is possible by printing at very low cost [125].

A number of *hybrid transparent conductors* have attracted attention during recent years; they combine at least two of the options discussed earlier. One may include the oxide/metal/oxide coatings in this class, provided that the oxide is a transparent conductor in its own right. Other alternatives of this rapidly growing group of transparent conductors include silver nanowires combined with ITO films or nanoparticles or with carbon nanotubes, graphene and so on. Furthermore, *macroscopic metal meshes, grids and arrays* can be of interest, although they may lead to unwanted optical scattering.

1.4.4
Electrolytes: Some Examples

Three types of electrolytes are of importance for electrochromic devices: thin solid films, polymer layers and ionic liquids. Electrolytes are generally proprietary in devices, and little is known about the ones that are used in practice.

Concerning thin solid films, those of porous oxide can be made H^+ or Li^+ conducting by co-deposition, by chemical or electrochemical post-treatment or by

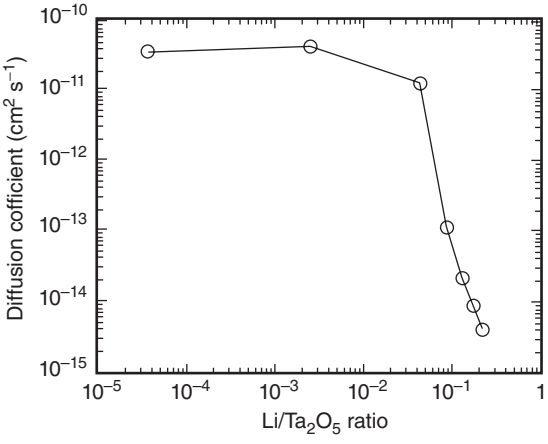

Figure 1.24 Diffusion coefficient for Ta oxide films with different amounts of Li^+. After Ref. [126].

exposure to humidity. A particularly well-studied example is tantalum pentoxide, whose applicability in electrochromic devices has been investigated in detail. For example, proton-conducting films have been prepared by sputter deposition of Ta in the presence of O_2 and H_2O and have shown an ion conductivity of $\sim 10^{-9}$ S cm^{-1} for as-deposited films; heat treatment led to a rapid decrease in their ion conductivity. Electrochemical lithium incorporation is another possibility and can yield amorphous-like films with Li^+ diffusion constants of 10^{-10} to 10^{-11} cm^2 s^{-1}, at least for Li/Ta_2O_5 ratios below 0.01, as evidenced in Figure 1.24, which reproduces data from Frenning *et al.* [126]. More complex thin-film electrolytes have been investigated in other work, such as LiPON [127] and $LiBO_2 - Li_2SO_4$ (known as LiBSO) [128].

Polymers and ionic liquids can be used in electrochromic devices that are more rugged than those possible with thin-film ion conductors. There are almost innumerable options. *In situ* polymerisation may be required for sealing purposes, and research with this object has been reported for polymer electrolytes [129] and ionic-liquid-based gel electrolytes [130]. Polymer electrolytes are discussed further in Chapter 10.

1.5 Towards Devices

Electrochromic device technology has been under development for many years, as noted in Section 1.1.2. There may be several reasons why this development has taken so many years, one being that electrochromic operation is 'difficult' and combines electrochemistry with optical technology and often also with

thin-film science in order to produce devices that should work for decades under harsh conditions while being observed by persons used to benchmarking against today's high-quality optical products (such as windows). Section 1.5.1 below considers a number of hurdles that must be overcome in order to have functional EC 'smart' windows. Section 1.5.2 then surveys some practical oxide-based devices. More in-depth discussions of device performance are presented elsewhere in this book.

1.5.1
Six Hurdles for Device Manufacturing

The first hurdle is that the electrochromic and the counter electrode films, shown in Figure 1.1, must have well-developed *nanoporosity* over their full areas, which may require that thin films are produced under non-standard conditions. These aspects were treated briefly in Section 1.3.5.

Secondly, the *transparent conductors* connecting electrochromic and counter electrode films must combine excellent electrical conductivity and high optical transparency, which is demanding particularly for polymer substrates. Transparent conductors of several different types were discussed in Sections 1.4.1 – 1.4.3.

The third difficulty is easily understood by considering the electrochromic device as a thin-film battery, which highlights that *charge insertion/extraction and charge balancing* are essential. In practical manufacturing, these processes must be accomplished by highly controllable and industrially viable techniques. Ozone exposure is one of several possible techniques [49, 131, 132].

Fourth, the *electrolyte* in the centre of the electrochromic device must combine good ion conductivity with very low electronic conductivity and high durability under solar irradiation. In some devices, it must also serve as an adhesive and reliably join two parts of the device.

Long-term *cycling durability* is of obvious interest for most electrochromic devices and is the fifth item. It hinges on good strategies for voltage and current control, which points at analogies between electrochromics and electrical batteries. These strategies, and their implementations via electronic drive circuitry design, are another area where proprietary considerations are dominating. However, it is evident that simple switching of voltage levels between two set values is far from an optimised strategy.

The sixth and final item is *large-scale manufacturability,* which is an obvious key to cost-effective electrochromic devices and hence to their acceptance on the consumer market. Clearly, it is necessary to avoid time-consuming production steps such as protracted thin-film deposition, long post-treatment times, elaborate steps for electrochemical charge insertion and extraction and so on. Life-cycle assessment is an important ingredient for judging the suitability of a specific manufacturing technology [133, 134]; these aspects are discussed in Chapter 18.

1.5.2 Practical Constructions of Electrochromic Devices

An uncritical reading of the scientific and technical literature may give an impression that many types of oxide-based electrochromic devices are available, but few of these are ready for practical use. However, there are some full-scale products and prototypes, especially for 'smart window' applications [115, 135–137], and those currently (2014) delivered to early adopters and other customers are introduced next. This presentation also allows a view of practical device designs and some insights into their pros and cons. The following literature references are to scientific journals, and some of these papers are rather old and probably more or less outdated. Thin films of tungsten oxide are a significant part of the electrochromic functionality for all of these devices.

We first consider a *five-layer 'monolithic' design* based on a single glass pane and developed by Sage Electrochromics Inc. in the United States [138] and Saint-Gobain Recherche in France [139]. Details are obscure, but it is clear that the electrolyte is a thin solid film. Such an arrangement makes it hard to avoid some leakage current between the electrochromic films through structural imperfections, and repeated electrical 'refresh' pulses may be needed to maintain the device in its dark state and transmittance changes can develop unevenly over large surfaces. The design may also lead to visible 'pin holes'. A related construction was developed by the US company View (earlier known as Soladigm Inc.). Somewhat analogous work was performed at the Optical Coating Laboratory Inc. (OCLI) in the United States during the 1990s [140, 141].

A laminated design embodying two double-layer-coated glass panes, joined by a polymer electrolyte, has been developed by Flabeg/EControl Glass GmbH in Germany. Some data are available for this device [142]. The electrolyte is injected in fluid form in a millimetre-wide gap between the glass panes via vacuum filling [143].

Another laminated device has been presented by Gesimat GmbH in Germany [144]. Here, the electrolyte is based on poly vinyl butyral (PVB), which is a standard material for glass lamination, and the transparent electrical conductors are produced by low-cost spray pyrolysis during float-glass production. The complementary electrochromic material is a film of iron(III) hexacyanoferrate(II) ('ferric ferrocyanide' or 'Prussian Blue'; see Chapter 2) prepared by electrodeposition.

A principally different *polymer-foil-based laminated design* has been developed by ChromoGenics AB in Sweden. It employs flexible PET foil substrates and allows roll-to-roll web coating [33, 145], that is, production by low-cost technology [146]. Another distinguishing feature is that the foil-based electrochromic device allows 'free-form design', which implies that product definition can be made at a later stage of device manufacturing. One PET foil is coated with a transparent and electrically conducting thin film and W oxide, another PET foil is coated with a transparent conductor and Ni oxide and the electrochromic-film-coated surfaces of the two foils are joined by an electrolyte via continuous lamination with an adhesive polymer. This type of electrochromic foil is discussed in more detail in Chapter 17.

1.6 Conclusions

This chapter has presented the conceptual and materials-oriented basis of oxide-based electrochromics with special attention to thin films of tungsten oxide and nickel oxide. The connection to the electronic properties and to nanostructural features was emphasised, and the importance of the thin-film manufacturing technology was stressed. Transparent electrical conductors and electrolytes were discussed too as were some general manufacturing aspects.

The electrochromic properties of a number of transition metal oxides have been known for decades and their application in devices have been attempted for many years. Promises of applications in 'smart windows' and elsewhere have been made repeatedly by many, but few products have emerged some products have swiftly been retracted. Nevertheless, research and development have progressed at a steady pace, and oxide-based electrochromic technology may finally (2015) be ready for market introduction on a massive scale.

Acknowledgement

Financial support during the writing of this chapter was received from the European Research Council under the European Community's Seventh Framework Program (FP7/2007–2013)/ERC Grant Agreement No. 267234 (GRINDOOR).

References

1. Granqvist, C.G. (1995) *Handbook of Inorganic Electrochromic Oxides*, Elsevier, Amsterdam.
2. Deb, S.K. (1995) Reminiscences on the discovery of electrochromic phenomena in transition metal oxides. *Sol. Energy Mater. Sol. Cells*, **39**, 191–201.
3. Andersson, A.M., Granqvist, C.G., and Stevens, J.R. (1989) Electrochromic Li_xWO_3/polymer laminate/$Li_yV_2O_5$ device: toward an all-solid-state smart window. *Appl. Opt.*, **28**, 3295–3302.
4. Passerini, S., Scrosati, B., Gorenstein, A., Andersson, A.M., and Granqvist, C.G. (1989) An electrochromic window based on Li_xWO_3/$(PEO)_8LiClO_4$/NiO. *J. Electrochem. Soc.*, **136**, 3394–3395.
5. Lampert, C.M. (2003) Large-area smart glass and integrated photovoltaics. *Sol. Energy Mater. Sol. Cells*, **76**, 489–499.
6. Fahlteich, J., Fahland, M., Schönberger, W., and Schiller, N. (2009) Permeation barrier properties of thin oxide films on flexible polymer substrates. *Thin Solid Films*, **517**, 3075–3080.
7. Rönnow, D., Kullman, L., and Granqvist, C.G. (1996) Spectroscopic light scattering from electrochromic tungsten-oxide-based films. *J. Appl. Phys.*, **80**, 423–430.
8. Deb, S.K. (1969) A novel electrophotographic system. *Appl. Opt. Suppl.*, **3**, 192–195.
9. Deb, S.K. (1973) Optical and photoelectric properties and colour centres in thin films of tungsten oxide. *Philos. Mag.*, **27**, 801–822.
10. Deb, S.K. (1992) Opportunities and challenges of electrochromic phenomena in transition metal oxides. *Sol. Energy Mater. Sol. Cells*, **25**, 327–338.
11. Svensson, J.S.E.M. and Granqvist, C.G. (1986) Electrochromic hydrated nickel oxide coatings for energy efficient

windows: optical properties and coloration mechanism. *Appl. Phys. Lett.*, **49**, 1566–1568.

12. Estrada, W., Andersson, A.M., and Granqvist, C.G. (1988) Electrochromic nickel-oxide-based coatings made by reactive dc magnetron sputtering: preparation and optical properties. *J. Appl. Phys.*, **64**, 3678–3683.
13. Palatnik, L.S., Malyuk, Y.I., and Belozerov, V.V. (1974) An X-ray diffraction study of the mechanism of reversible electrochemical dielectric ↔ semiconductor transformations in Nb_2O_5. *Dokl. Akad. Nauk SSSR*, **215**, 1182–1185 [English translation: *Dokl. Chem. Technol.*, **215** (5), 68–71].
14. de Vries, G.C. (1999) Electrochromic variable transmission glass for picture tubes. *Electrochim. Acta*, **44**, 3185–3193.
15. Baloukas, B., Lamarre, J.-M., and Martinu, L. (2011) Active metameric security devices using an electrochromic material. *Appl. Opt.*, **50**, C41–C49.
16. Baucke, F.G.K. (1991) Electrochromic applications. *Mater. Sci. Eng., B*, **10**, 285–292.
17. Byker, H.J. (1994) in *Proceedings of the Symposium on Electrochromic Materials II* (eds K.-C. Ho and D.A. MacArthur), The Electrochemical Society, Pennington, NJ, pp. 3–13.
18. Lampert, C.M. (1984) Electrochromic materials and devices for energy efficient windows. *Sol. Energy Mater.*, **11**, 1–27.
19. Svensson, J.S.E.M. and Granqvist, C.G. (1984) Electrochromic tungsten oxide films for energy efficient windows. *Sol. Energy Mater.*, **11**, 29–34.
20. Svensson, J.S.E.M. and Granqvist, C.G. (1985) Electrochromic coatings for "smart windows". *Sol. Energy Mater.*, **12**, 391–402.
21. Svensson, J.S.E.M. and Granqvist, C.G. (1985) Electrochromic coatings for smart windows: crystalline and amorphous WO_3 films. *Thin Solid Films*, **126**, 31–36.
22. Ma, C., Taya, M., and Xu, C. (2008) Smart sunglasses based on electrochromic polymers. *Polym. Eng. Sci.*, **48**, 2224–2228.
23. Buyan, M., Brühwiler, P.A., Azens, A., Gustavsson, G., Karmhag, R., and Granqvist, C.G. (2006) Facial warming and tinted helmet visors. *Int. J. Ind. Ergon.*, **36**, 11–16.
24. Demiryont, H. and Moorehead, D. (2009) Electrochromic emissivity modulator for spacecraft thermal management. *Sol. Energy Mater. Sol. Cells*, **93**, 2075–2078.
25. Metts, J.G., Nabity, J.A., and Klaus, D.M. (2011) Theoretical performance analysis of electrochromic radiators for space suit thermal control. *Adv. Space Res.*, **47**, 1256–1264.
26. Teissier, A., Dudon, J.-P., Aubert, P.-H., Vidal, F., Remaury, S., Crouzet, J., and Chevrot, C. (2012) Feasibility of conducting semi-IPN with variable electro-emissivity: a promising way for spacecraft thermal control. *Sol. Energy Mater. Sol. Cells*, **99**, 116–122.
27. Sauvet, K., Sauques, L., and Rougier, A. (2009) IR electrochromic WO_3 thin films: from optimization to devices. *Sol. Energy Mater. Sol. Cells*, **93**, 2045–2049.
28. Brown, R.M. and Hillman, A.R. (2012) Electrochromic enhancement of latent fingerprints by poly(3,4-ethylenedioxythiophene). *Phys. Chem. Chem. Phys.*, **14**, 8653–8661.
29. Invernale, M.A., Ding, Y., and Sotzing, G.A. (2010) All-organic electrochromic spandex. *ACS Appl. Mater. Interfaces*, **2**, 296–300.
30. Granqvist, C.G. (2000) Electrochromic tungsten oxide films: review of progress 1993–1998. *Sol. Energy Mater. Sol. Cells*, **60**, 201–262.
31. Granqvist, C.G., Avendaño, E., and Azens, A. (2003) Electrochromic coatings and devices: survey of some recent advances. *Thin Solid Films*, **442**, 201–211.
32. Granqvist, C.G. (2007) Transparent conductors as solar energy materials: a panoramic review. *Sol. Energy Mater. Sol. Cells*, **91**, 1529–1598.

33. Niklasson, G.A. and Granqvist, C.G. (2007) Electrochromics for smart windows: thin films of tungsten oxide and nickel oxide, and devices based on these. *J. Mater. Chem.*, **17**, 127–156.
34. Granqvist, C.G., Azens, A., Heszler, P., Kish, L.B., and Österlund, L. (2007) Nanomaterials for benign indoor environments: electrochromics for "smart windows", sensors for air quality, and photo-catalysis for air cleaning. *Sol. Energy Mater. Sol. Cells*, **91**, 355–365.
35. Pulker, H. (1999) *Coatings on Glass*, 2nd edn, Elsevier, Amsterdam.
36. Gläser, H.J. (2000) *Large Area Glass Coating*, von Ardenne Anlagentechnik, Dresden.
37. Ohring, M. (2002) *The Materials Science of Thin Films: Deposition and Structure*, 2nd edn, Academic Press, New York.
38. Mattox, D.M. (2010) *Handbook of Physical Vapor Deposition (PVD) Processing*, 2nd edn, Elsevier/William Andrew, Norwich, NY.
39. Granqvist, C.G. (2012) Preparation of thin films and nanostructured coatings for clean tech applications: a primer. *Sol. Energy Mater. Sol. Cells*, **99**, 166–175.
40. Piegari, A. and Flory, F. (2013) *Optical Thin Films and Coatings: From Materials to Applications*, Woodhead, Cambridge.
41. Zheng, H., Ou, J.Z., Strano, M.S., Kaner, R.B., Mitchell, A., and Kalantar-zadeh, K. (2011) Nanostructured tungsten oxide: properties, synthesis, and applications. *Adv. Funct. Mater.*, **21**, 2175–2196.
42. Hashimoto, S. and Matsuoka, H. (1991) Lifetime of electrochromism of amorphous WO_3–TiO_2 thin films. *J. Electrochem. Soc.*, **138**, 2403–2408.
43. Göttsche, J., Hinsch, A., and Wittwer, V. (1993) Electrochromic mixed WO_3–TiO_2 thin films produced by sputtering and the sol–gel technique: a comparison. *Sol. Energy Mater. Sol. Cells*, **31**, 415–428.
44. Lin, F., Cheng, J., Engtrakul, C., Dillon, A.C., Nordlund, D., Moore, R.G., Weng, T.-C., Williams, S.K.R., and Richards, R.M. (2012) *In situ* crystallization of high performing WO_3-based electrochromic materials and the importance for durability and switching kinetics. *J. Mater. Chem.*, **22**, 16817–16823.
45. Ramana, C.V., Baghmar, G., Rubio, E.J., and Hernandez, M.J. (2013) Optical constants of amorphous, transparent titanium-doped tungsten oxide thin films. *ACS Appl. Mater. Interfaces*, **5**, 4659–4666.
46. Manciu, F.S., Yun, Y., Durrer, W.G., Howard, J., Schmidt, U., and Ramana, C.V. (2012) Comparative microscopic and spectroscopic analysis of temperature-dependent growth of WO_3 and $W_{0.95}Ti_{0.05}O_3$ thin films. *J. Mater. Sci.*, **47**, 6593–6600.
47. Avendaño, E., Azens, A., Niklasson, G.A., and Granqvist, C.G. (2004) Electrochromism in nickel oxide films containing Mg, Al, Si, V, Zr, Nb, Ag, or Ta. *Sol. Energy Mater. Sol. Cells*, **84**, 337–350.
48. Gillaspie, D., Norman, A., Tracy, C.E., Pitts, J.R., Lee, S.-H., and Dillon, A. (2010) Nanocomposite counter electrode materials for electrochromic windows. *J. Electrochem. Soc.*, **157**, H328–H331.
49. Lin, F., Nordlund, D., Weng, T.-C., Moore, R.G., Gillaspie, D.T., Dillon, A.C., Richards, R.M., and Engtrakul, C. (2013) Hole doping in Al-containing nickel oxide materials to improve electrochromic performance. *ACS Appl. Mater. Interfaces*, **5**, 301–309.
50. Lin, F., Nordlund, D., Weng, T.-C., Sokaras, D., Jones, K.M., Reed, R.B., Gillaspie, D.T., Weir, D.G., Moore, R.G., Dillon, A.C., Richards, R.M., and Engtrakul, C. (2013) Origin of electrochromism in high-performing nanocomposite nickel oxide. *ACS Appl. Mater. Interfaces*, **5**, 3643–3649.
51. Cha, I.Y., Park, S.H., Lim, J.W., Yoo, S.J., and Sung, Y.-E. (2013) The activation process through a bimodal transmittance state for improving electrochromic performance of nickel oxide thin film. *Sol. Energy Mater. Sol. Cells*, **108**, 22–26.
52. Burdis, M.S., Siddle, J.R., Batchelor, R.A., and Gallego, J.M. (1998)

$V_{0.50}Ti_{0.50}O_x$ thin films as counter-electrodes for electrochromic devices. *Sol. Energy Mater. Sol. Cells*, **54**, 93–98.

53. Marcel, C., Brigouleix, C., Vincent, A., Plessis, D., Nouhaud, G., Hamon, Y., Sabary, F., and Campet, G. (2003) in *Electrochromic Materials and Applications* (eds A. Rougier, D. Rauh, and G.A. Nazri), The Electrochemical Society, Pennington, NJ, pp. 218–230.
54. Granqvist, C.G. (1994) Electrochromic oxides: a unified view. *Solid State Ion.*, **70/71**, 678–685.
55. Enjalbert, R. and Galy, J. (1986) A refinement of the structure of V_2O_5. *Acta Crystallogr., Sect. C*, **42**, 1467–1469.
56. Haber, J., Witko, M., and Tokarz, R. (1997) Vanadium pentoxide I: structures and properties. *Appl. Catal., A*, **157**, 3–22.
57. Avendaño, E., Azens, A., Niklasson, G.A., and Granqvist, C.G. (2005) Proton diffusion and electrochromism in hydrated NiO_y and $Ni_{1-x}V_xO_y$ thin films. *J. Electrochem. Soc.*, **152**, F203–F205.
58. Avendaño, E., Rensmo, H., Azens, A., Sandell, A., Azevedo, G.d.M., Siegbahn, H., Niklasson, G.A., and Granqvist, C.G. (2009) Coloration mechanism in proton-intercalated hydrated NiO_y and $Ni_{1-x}V_xO_y$ thin films. *J. Electrochem. Soc.*, **156**, P132–P138.
59. Goodenough, J.B. (1971) in *Progress in Solid State Chemistry*, vol. **5** (ed H. Reiss), Pergamon, Oxford, pp. 145–399.
60. Talledo, A. and Granqvist, C.G. (1995) Electrochromic vanadium-pentoxide-based films: structural, electrochemical, and optical properties. *J. Appl. Phys.*, **77**, 4655–4666.
61. Gavrilyuk, A., Tritthart, U., and Gey, W. (2011) Photoinjection of hydrogen and the nature of a giant shift of the fundamental absorption edge in highly disordered V_2O_5 films. *Phys. Chem. Chem. Phys.*, **13**, 9490–9497.
62. Schirmer, O.F., Wittwer, V., Baur, G., and Brandt, G. (1977) Dependence of WO_3 electrochromic absorption on crystallinity. *J. Electrochem. Soc.*, **124**, 749–753.
63. Bryksin, V.V. (1982) Optical intraband absorption in disordered systems with strong electron–phonon interaction. *Fiz. Tverd. Tela*, **24**, 1110–1117 [English translation: *Sov. Phys. Solid State*, **24**, 627–631].
64. He, T. (1995) Optical absorption of free small polarons at high temperatures. *Phys. Rev. B*, **51**, 16689–16694.
65. Berggren, L., Azens, A., and Niklasson, C.G. (2001) Polaron absorption in amorphous tungsten oxide films. *J. Appl. Phys.*, **90**, 1860–1863.
66. Faughnan, B.W., Crandall, R.S., and Heyman, P.M. (1975) Electrochromism in WO_3 amorphous films. *RCA Rev.*, **36**, 177–197.
67. Gabrusenoks, J.V., Cikmach, P.D., Lusis, A.R., Kleperis, J.J., and Ramans, G.M. (1984) Electrochromic colour centres in amorphous tungsten trioxide thin films. *Solid State Ion.*, **14**, 25–30.
68. Saenger, M.F., Höing, T., Hofmann, T., and Schubert, M. (2008) Polaron transitions in charge intercalated amorphous tungsten oxide thin films. *Phys. Status Solidi A*, **205**, 914–917.
69. Denesuk, M. and Uhlmann, D.R. (1996) Site-saturation model for the optical efficiency of tungsten-oxide-based devices. *J. Electrochem. Soc.*, **143**, L186–L188.
70. Berggren, L. and Niklasson, G.A. (2006) Optical charge transfer absorption in lithium-intercalated tungsten oxide thin films. *Appl. Phys. Lett.*, **88**, 081906/1–081906/3.
71. Berggren, L., Jonsson, J.C., and Niklasson, G.A. (2007) Optical absorption in lithiated tungsten oxide thin films: experiments and theory. *J. Appl. Phys.*, **102**, 083538/1–083538/7.
72. Yamada, Y., Tajima, K., Bao, S., Okada, M., and Yoshimura, K. (2009) Optical charge transfer absorption in proton injected tungsten oxide thin films analyzed with spectroscopic ellipsometry. *Solid State Ion.*, **180**, 659–661.
73. Balaji, S., Djaoued, Y., Albert, A.-S., Ferguson, R.Z., and Brüning, R. (2009) Hexagonal tungsten oxide based electrochromic devices: spectroscopic evidence for the Li ion occupancy

of four-coordinated square windows. *Chem. Mater.*, **21**, 1381–1389.

74. Kharade, R.R., Patil, K.R., Patil, P.S., and Bhosale, P.N. (2012) Novel microwave assisted sol–gel synthesis (MW-SGS) and electrochromic performance of petal like *h*-WO_3 thin films. *Mater. Res. Bull.*, **47**, 1787–1793.
75. Nanba, T. and Yasui, I. (1989) X-ray diffraction study of microstructure of amorphous tungsten trioxide films prepared by electron beam vacuum evaporation. *J. Solid State Chem.*, **83**, 304–315.
76. Thornton, J.A. (1977) High-rate thin film growth. *Annu. Rev. Mater. Sci.*, **7**, 239–260.
77. Sun, X., Liu, Z., and Cao, H. (2010) Effects of film density on electrochromic tungsten oxide thin films deposited by reactive dc-pulsed magnetron sputtering. *J. Alloys Compd. (Suppl.)*, **504S**, S418–S421.
78. Le Bellac, D., Azens, A., and Granqvist, C.G. (1995) Angular selective transmittance through electrochromic tungsten oxide films made by oblique angle sputtering. *Appl. Phys. Lett.*, **66**, 1715–1716.
79. Beydaghyan, G., Renaud, J.-L.M., Bader, G., and Ashrit, P.V. (2008) Enhanced electrochromic properties of heat treated nanostructured tungsten trioxide thin films. *J. Mater. Res.*, **23**, 274–280.
80. Gil-Rostra, J., Cano, M., Pedrosa, J.M., Ferrer, J.F., García-García, F., Yubero, F., and González-Elipe, A.R. (2011) Electrochromic behavior of $W_xSi_yO_z$ thin films prepared by reactive magnetron sputtering at normal and glancing angles. *ACS Appl. Mater. Interfaces*, **4**, 628–638.
81. Nagata, S., Fujita, H., Inouye, A., Yamamoto, S., Tsuchiya, B., and Shikama, T. (2010) Ion irradiation effects on the optical properties of tungsten oxide films. *Nucl. Instrum. Methods Phys. Res., Sect. B*, **268**, 3151–3154.
82. Sai, L., Tang, L., Huang, X., Chen, G., Zhao, J., and Wang, J. (2012) Lowest-energy structures of $(WO_3)_n$ ($2 \leq n \leq 12$) clusters from first-principles global search. *Chem. Phys. Lett.*, **544**, 7–12.
83. Maleknia, S., Brodbelt, J., and Pope, K. (1991) Characterization of the reactive and dissociative behavior of transition metal oxide cluster ions in the gas phase. *J. Am. Soc. Mass Spectrom.*, **2**, 212–219.
84. Lang, Z.-L., Guan, W., Yan, L.-K., Wen, S.-Z., Su, Z.-M., and Hao, L.-Z. (2012) The self-assembly mechanism of the Lindqvist anion $[W_6O_{19}]^{2-}$ in aqueous solution: a density functional theory study. *Dalton Trans.*, **41**, 11361–11368.
85. Sorar, I., Pehlivan, E., Niklasson, G.A., and Granqvist, C.G. (2013) Electrochromism of DC magnetron sputtered TiO_2 thin films: role of deposition parameters. *Sol. Energy Mater. Sol. Cells*, **115**, 172–180.
86. Sorar, I., Pehlivan, E., Niklasson, G.A., and Granqvist, C.G. (2014) Electrochromism of DC magnetron-sputtered TiO_2: role of film thickness. *Appl. Surf. Sci.*, **318**, 24–27.
87. Green, S.V., Watanabe, M., Oka, N., Niklasson, G.A., Granqvist, C.G., and Shigesato, Y. (2012) Electrochromic properties of nickel oxide based thin films sputter deposited in the presence of water vapor. *Thin Solid Films*, **520**, 3839–3842.
88. Ueta, H., Abe, Y., Kato, K., Kawamura, M., Sasaki, K., and Itoh, H. (2009) Ni oxyhydroxide thin films prepared by reactive sputtering using $O_2 + H_2O$ mixed gas. *Jpn. J. Appl. Phys.*, **48**, 015501/1–015501/4.
89. Abe, Y., Ueta, H., Obata, T., Kawamura, M., Sasaki, K., and Itoh, H. (2010) Effects of sputtering gas pressure on electrochromic properties of Ni oxyhydroxide thin films prepared by reactive sputtering in H_2O atmosphere. *Jpn. J. Appl. Phys.*, **49**, 115802/1–115802/4.
90. Yuan, Y.F., Xia, X.H., Wu, J.B., Chen, Y.B., Yang, J.L., and Guo, S.Y. (2011) Enhanced electrochromic properties of ordered porous nickel oxide thin film prepared by self-assembled colloidal crystal template-assisted electrodeposition. *Electrochim. Acta*, **56**, 1208–1212.

91. Oka, N., Watanabe, M., Sugie, K., Iwabuchi, Y., Kotsubo, H., and Shigesato, Y. (2013) Reactive-gas-flow sputter deposition of amorphous WO_3 films for electrochromic devices. *Thin Solid Films*, **532**, 1–6.
92. Hemberg, A., Dauchot, J.-P., Snyders, R., and Konstantinidis, S. (2012) Evaporation-assisted high-power impulse magnetron sputtering: the deposition of tungsten oxide as a case study. *J. Vac. Sci. Technol., A*, **30**, 040604/1–040604/4.
93. Green, S.V., Kuzmin, A., Purans, J., Granqvist, C.G., and Niklasson, G.A. (2011) Structure and composition of sputter-deposited nickel–tungsten oxide films. *Thin Solid Films*, **519**, 2062–2066.
94. Green, S.V., Pehlivan, E., Granqvist, C.G., and Niklasson, G.A. (2012) Electrochromism in sputter deposited nickel-oxide films. *Sol. Energy Mater. Sol. Cells*, **99**, 339–344.
95. Green, S.V. (2012) *Electrochromic Nickel–Tungsten Oxides: Optical, Electrochemical and Structural Characterization of Sputter-Deposited Thin Films in the Whole Composition Range*, Digital Comprehensive Summaries of Uppsala Dissertations from the Faculty of Science and Technology, vol. **963**, Acta Universitatis Upsaliensis, Uppsala, ISBN 978-91-554-8444-6.
96. Green, S.V., Granqvist, C.G., and Niklasson, G.A. (2014) Structure and optical properties of electrochromic tungsten-containing nickel oxide films. *Sol. Energy Mater. Sol. Cells*, **126**, 248–259.
97. Valyukh, I., Green, S.V., Granqvist, C.G., Niklasson, G.A., Valyukh, S., and Arwin, H. (2011) Optical properties of thin films of mixed Ni–W oxide made by reactive DC magnetron sputtering. *Thin Solid Films*, **519**, 2914–2918.
98. Valyukh, I., Green, S.V., Granqvist, C.G., Gunnarsson, K., Arwin, H., and Niklasson, G.A. (2012) Ellipsometrically determined optical properties of nickel-containing tungsten oxide thin films: nanostructure inferred from effective medium theory. *J. Appl. Phys.*, **112**, 044308/1–044308/6.
99. Ellmer, K., Klein, A., and Rech, B. (eds) (2008) *Transparent Conductive Zinc Oxide: Basics and Applications*, Springer, Berlin.
100. Ginley, D.S., Hosono, H., and Paine, D.C. (eds) (2010) *Handbook of Transparent Conductors*, Springer Science+Business Media, New York.
101. Ellmer, K. (2012) Past achievements and future challenges in the development of optically transparent electrodes. *Nat. Photonics*, **6**, 809–817.
102. WINDOW International Glazing Database, Lawrence Berkeley National Laboratory, Berkeley, CA, *http://windows.lbl.gov/software/window/window.html* (accessed 19 February 2015).
103. Hamberg, I. and Granqvist, C.G. (1986) Evaporated Sn-doped In_2O_3 films: basic optical properties and applications to energy-efficient windows. *J. Appl. Phys.*, **60**, R123–R159.
104. Jin, Z.-C. and Granqvist, C.G. (1988) Optical properties of sputter-deposited ZnO:Al thin films. *J. Appl. Phys.*, **64**, 5117–5131.
105. Stjerna, B., Olsson, E., and Granqvist, C.G. (1994) Optical and electrical properties of radio frequency sputtered tin oxide films doped with oxygen vacancies, F, Sb, or Mo. *J. Appl. Phys.*, **76**, 3707–3817.
106. Cairns, D.R., Witte, R.P. II,, Sparacin, D.K., Sachsman, S.M., Paine, D.C., Crawford, G.P., and Newton, R.R. (2000) Strain-dependent electrical resistance of tin-doped indium oxide on polymer substrates. *Appl. Phys. Lett.*, **76**, 1425–1427.
107. Kim, E.-H., Yang, C.-W., and Park, J.-W. (2011) The crystallinity and mechanical properties of indium tin oxide coatings on polymer substrates. *J. Appl. Phys.*, **109**, 043511/1–043511/8.
108. Schwartz-Schampera, U. and Herzig, P.M. (2002) *Indium: Geology, Mineralogy, and Economics*, Springer, Berlin.
109. Cummings, K.J., Nakano, M., Omae, K., Takeuchi, K., Chonan, T., Xiao, Y.-L., Harley, R.A., Roggli, V.L., Hebisawa, A., Tallaksen, R.J., Trapnell, B.C., Day, G.A., Saito, R., Stanton, M.L.,

Suarthana, E., and Kreiss, K. (2012) Indium lung disease. *Chest*, **141**, 1512–1521.

110. Ostermann, R. and Smarsly, B. (2009) Does mesoporosity enhance thin film properties? A question of electrode material for electrochromism of WO_3. *Nanoscale*, **1**, 266–270.

111. Smith, G.B., Niklasson, G.A., Svensson, J.S.E.M., and Granqvist, C.G. (1986) Noble-metal-based transparent infrared reflectors: experiments and theoretical analyses for very thin gold films. *J. Appl. Phys.*, **59**, 571–581.

112. Hövel, M., Gompf, B., and Dressel, M. (2010) Dielectric properties of ultrathin films around the percolation threshold. *Phys. Rev. B*, **81**, 035402/1–035402/8.

113. Lansåker, P.C., Backholm, J., Niklasson, G.A., and Granqvist, C.G. (2009) TiO_2/Au/TiO_2 multilayer thin films: novel metal-based transparent conductors for electrochromic devices. *Thin Solid Films*, **518**, 1225–1229.

114. Smith, G.B. and Granqvist, C.G. (2010) *Green Nanotechnology: Solutions for Sustainability and Energy in the Built Environment*, CRC Press, Boca Raton, FL.

115. Jelle, B.P. (2013) Solar radiation glazing factors for window panes, glass structures and electrochromic windows in buildings: measurement and calculation. *Sol. Energy Mater. Sol. Cells*, **116**, 291–323.

116. Roth, S. and Park, H.J. (2010) Nanocarbonic transparent conductive films. *Chem. Soc. Rev.*, **39**, 2477–2483.

117. Niu, C. (2011) Carbon nanotube transparent conducting films. *MRS Bull.*, **36**, 766–773.

118. Feng, C., Liu, K., Wu, J.-S., Liu, L., Cheng, J.-S., Zhang, Y., Sun, Y., Li, Q., Fan, S., and Jiang, K. (2010) Flexible, stretchable, transparent conducting films made from superaligned carbon nanotubes. *Adv. Funct. Mater.*, **20**, 885–891.

119. Novoselov, K.S., Fal'ko, V.I., Colombo, L., Gellert, P.R., Schwab, M.G., and Kim, K. (2012) A roadmap for graphene. *Nature*, **490**, 192–200.

120. De, S., King, P.J., Lotya, M., O'Neill, A., Doherty, E.M., Hernandez, Y., Duesberg, G.S., and Coleman, J.N. (2010) Flexible, transparent, conducting films of randomly stacked graphene from surfactant-stabilized, oxide-free graphene dispersions. *Small*, **6**, 458–464.

121. De Arco, L.G., Zhang, Y., Schlenker, C.W., Ryu, K., Thompson, M.E., and Zhou, C. (2010) Continuous, highly flexible, and transparent graphene films by chemical vapor deposition for organic photovoltaics. *ACS Nano*, **4**, 2865–2873.

122. Bae, S., Kim, H., Lee, Y., Xu, X., Park, J.-S., Zheng, Y., Balakrishnan, J., Lei, T., Kim, H.R., Song, Y.I., Kim, Y.-J., Kim, K.S., Özyilmaz, B., Ahn, J.-H., Hong, B.H., and Iijima, S. (2010) Roll-to-roll production of 30-inch graphene films for transparent electrodes. *Nat. Nanotechnol.*, **5**, 574–578.

123. Wu, H., Kong, D., Ruan, Z., Hsu, P.-C., Wang, S., Yu, Z., Carney, T.J., Hu, L., Fan, S., and Cui, Y. (2013) A transparent electrode based on a metal nanotrough network. *Nat. Nanotechnol.*, **8**, 421–425.

124. Preston, C., Xu, Y., Han, X., Munday, J.N., and Hu, L. (2013) Optical haze of transparent and conductive silver nanowire films. *Nano Res.*, **6**, 461–468.

125. Elschner, A. and Lövenich, W. (2011) Solution-deposited PEDOT for transparent conductive applications. *MRS Bull.*, **36**, 794–798.

126. Frenning, G., Engelmark, F., Niklasson, G.A., and Strømme, M. (2001) Li conduction in sputtered amorphous Ta_2O_5. *J. Electrochem. Soc.*, **148**, A418–A421.

127. Yoo, S.J., Lim, J.W., and Sung, Y.-E. (2006) Improved electrochromic devices with an inorganic solid electrolyte protective layer. *Sol. Energy Mater. Sol. Cells*, **90**, 477–484.

128. Yang, H., Wang, C., Diao, X., Wang, H., Wang, T., and Zhu, K. (2008) A new all-thin-film electrochromic device using LiBSO as the ion conducting layer. *J. Phys. D Appl. Phys.*, **41**, 115301/1–115301/5.

129. Soutar, A.M., Rosseinsky, D.R., Freeman, W., Zhang, X., How, X., Jiang, H., Zeng, X., and Miso, X. (2012) Electrochromic cell with UV-curable

electrolyte polymer for cohesion and strength. *Sol. Energy Mater. Sol. Cells*, **100**, 268–270.

130. Sydam, R., Deepa, M., and Srivastava, A.K. (2012) Electrochromic device response controlled by an *in situ* polymerized ionic liquid based gel electrolyte. *RSC Adv.*, **2**, 9011–9021.

131. Azens, A., Kullman, L., and Granqvist, C.G. (2003) Ozone coloration of Ni and Cr oxide films. *Sol. Energy Mater. Sol. Cells*, **76**, 147–153.

132. Aydogdu, G.H., Ruzmetov, D., and Ramanathan, S. (2010) Metastable oxygen incorporation into thin film NiO by low temperature active oxidation: influence of hole conduction. *J. Appl. Phys.*, **108**, 113702/1–113702/6.

133. Papaefthimiou, S., Syrrakou, E., and Yianoulis, P. (2009) An alternative approach for the energy and environmental rating of advanced glazing: an electrochromic window case study. *Energy Build.*, **41**, 17–26.

134. Posset, U., Harsch, M., Rougier, A., Herbig, B., Schottner, G., and Sextl, G. (2012) Environmental assessment of electrically controlled variable light transmittance devices. *RSC Adv.*, **2**, 5990–5996.

135. Baetens, R., Jelle, B.P., and Gustavsen, A. (2010) Properties, requirements and possibilities of smart windows for dynamic daylight and solar energy control in buildings: a state-of-the-art review. *Sol. Energy Mater. Sol. Cells*, **94**, 87–105.

136. Granqvist, C.G. (2012) Oxide electrochromics: an introduction to devices and materials. *Sol. Energy Mater. Sol. Cells*, **99**, 1–13.

137. Jelle, B.P., Hynd, A., Gustavsen, A., Arasteh, D., Goudey, H., and Hart, R. (2012) Fenestration today and tomorrow: a state-of-the-art review and future research opportunities. *Sol. Energy Mater. Sol. Cells*, **96**, 1–28.

138. Sbar, N., Badding, M., Budziak, R., Cortez, K., Laby, L., Michalski, L., Ngo, T., Schulz, S., and Urbanik, K. (1999) Progress toward durable, cost effective electrochromic window glazings. *Sol. Energy Mater. Sol. Cells*, **56**, 321–341.

139. Béteille, F., Boire, P., and Giron, J.-C. (1999) Highly durable all-solid-state electrochromic glazings. *Proc. Soc. Photo-Opt. Instrum. Eng.*, **3788**, 70–74.

140. Mathew, J.G.H., Sapers, S.P., Cumbo, M.J., O'Brien, N.A., Sargent, R.B., Raksha, V.P., Lahaderne, R.B., and Hichwa, B.P. (1997) Large area electrochromics for architectural applications. *J. Non-Cryst. Solids*, **218**, 342–346.

141. O'Brien, N.A., Gordon, J., Mathew, H., and Hichwa, B.P. (1999) Electrochromic coatings: applications and manufacturing issues. *Thin Solid Films*, **345**, 312–318.

142. Zinzi, M. (2006) Office worker preferences of electrochromic windows: a pilot study. *Build. Environ.*, **41**, 1262–1273.

143. Xu, C., Ma, C., Kong, X., and Taya, M. (2009) Vacuum filling process for electrolyte in enhancing electrochromic polymer window assembly. *Polym. Adv. Technol.*, **20**, 178–182.

144. Kraft, A. and Rottman, M. (2009) Properties, performance and current status of the laminated electrochromic glass of Gesimat. *Sol. Energy Mater. Sol. Cells*, **93**, 2088–2092.

145. Azens, A., Gustavsson, G., Karmhag, R., and Granqvist, C.G. (2003) Electrochromic devices on polyester foil. *Solid State Ion.*, **165**, 1–5.

146. Bishop, C.A. (2011) *Vacuum Deposition onto Webs, Films, and Foils*, 2nd edn, William Andrew, Waltham, MA.